Report No. CDOT-DTD-R-94-3

Comparison of Test Results from Laboratory and Field Compacted Samples

J.D.Stevenson
FHWA, Colorado Division
555 Zang Street, Room 250
Lakewood, Co. 80228

Tim Aschenbrener
Colorado DOT
4340 East Louisiana Avenue
Denver, Co. 80222

Final Report
Febuary 1994

The contents of this report reflect the views of authors who are responsible for the facts and the accuracy of the data presented herein. The contents do not necessarily reflect the official views of the Colorado Department of Transportation or the Federal Highway Administration. This report does not constitute a standard, specification, or regulation.

Acknowledgements

The authors would like to express their gratitude to all of the project engineers who cooperated with our research study and allowed us to obtain samples for this investigation:
Van Pilaud (CDOT-Region 3), Robert Birch (CDOT-Region 6), Marv Bindel (CDOT-Region 6), Gerry Padilla (CDOT-Region 4), Kevin Albert (CDOT-Region 2), and Bob Chaderton (CDOT-Region 4). Dave Price (CDOT-Research) obtained the field samples and assisted with laboratory testing.

The CDOT research panel provided many excellent comments and suggestions for the study. It included: Byron Lord and Kevin Stuart (FHWA - Turner Fairbank Highway Research Center); Doyt Bolling (FHWA - Region 8), Jerry Cloud (FHWA - Colorado Division), Denis Donnelly and Steve Horton (CDOT-Staff Materials), Ken Wood (CDOT-Region 4 Materials), and Donna Harmelink (CDOT-Research).

Special thanks to the panel of Colorado asphalt paving experts who provided numerous ideas and suggestions which made this study more informational: Bud Brakey (Brakey Consulting Engineers), Jim Fife (Western Colorado Testing), Joe Proctor (Morton International), Scott Shuler (Colorado Asphalt Pavement Association) and Eric West (Western Mobile). Dr. Jack Corlew (Process Consultant) provided a technical review.

Technical Report Documentation Page

1. Report No.	2. Government Accession No.	3. Recipient's Catalog No.
CDOT-DTD-R-94-3		

4. Title and Subtitle	5. Report Date
Comparison of Test Results from Laboratory and Field Compacted Samples	February 1994
	6. Performing Organization Code
7. Author(s)	**8. Performing Organization Rpt.No.**
Timothy Aschenbrener	CDOT-DTD-R-94-3
9. Performing Organization Name and Address	**10. Work Unit No. (TRAIS)**
Colorado Department of Transportation 4201 E. Arkansas Ave. Denver, Colorado 80222	**11. Contract or Grant No.**
12. Sponsoring Agency Name and Address	**13. Type of Rpt. and Period Covered**
Colorado Department of Transportation 4201 E. Arkansas Ave. Denver, Colorado 80222	Final Report **14. Sponsoring Agency Code**

15. Supplementary Notes

Prepared in Cooperation with the U.S. Department of Transportation Federal Highway Administration

16. Abstract

Studies have been completed to verify the predictive capabilities of the testing equipment by performing tests on mixtures of known field performance. The Hamburg wheel-tracking device and the French rutting tester have the ability to model field performance very well.

The purpose of this report is to compare test results from the European testing equipment using laboratory and field compacted samples. The results from this study will be beneficial to 1) decide how close the laboratory compactors "simulate" field compaction, and 2) assist with the development of specifications for field acceptance testing.

When tested in the French rutting tester, samples compacted in the French plate compactor and linear kneading compactor produce samples that give very similar test results to field compacted samples. When tested in the Hamburg wheel-tracking device, results from the lab compacted samples indicated the mixes would be more resistant to moisture damage than the results from field compacted samples. The air voids in the field compacted samples were more uniformly distributed than in the lab compacted samples.

Implementation:

17. Key Words	18. Distribution Statement
	No Restrictions: This report is available to the public through the National Technical Info. Service. Springfield, VA 22161

19.Security Classif. (report)	20.Security Classif. (page)	21. No. of Pages	22. Price
Unclassified	Unclassified	92	

Table of Contents

List of Tables

List of Figures

Appendices

Comparison of Test Results from
Laboratory and Field Compacted Samples

J.D. Stevenson and Tim Aschenbrener

1.0 Introduction

In September 1990, a group of individuals representing AASHTO, FHWA, NAPA, SHRP, AI, and TRB participated in a 2-week tour of six European countries. Information on this tour has been published in a "Report on the 1990 European Asphalt Study Tour" (1). Several areas for potential improvement of hot mix asphalt (HMA) pavements were identified, including the use of performance-related testing equipment used in several European countries. The Colorado Department of Transportation (CDOT) and the FHWA Turner-Fairbank Highway Research Center (TFHRC) were selected to demonstrate this equipment.

Studies have been completed to verify the predictive capabilities of the testing equipment by performing tests on mixtures of known field performance. The Hamburg wheel-tracking device and the French rutting tester have the ability to model field performance very well. Samples are prepared for testing in the European equipment with laboratory compactors that are supposed to "simulate" field compaction. It was desired to compare how well the laboratory compactors modelled the actual field compaction using roadway construction equipment.

Additionally, it is desired to improve the quality of HMA on projects by using results from these tests as specifications. When accepting a laboratory mix design or a field produced material, it is not clear how the laboratory compaction process models the field compaction. By comparing field and laboratory compacted samples, information would be available to better prepare acceptance specifications.

The purpose of this report is to compare test results from the European testing equipment using laboratory and field compacted samples. The results from this study will be beneficial to 1) decide how close the laboratory compactors "simulate" field compaction, and 2) assist with the development of specifications for field acceptance testing.

2.0 Experimental Grid

2.1 Laboratory Tests

The tests used to compare field and laboratory compacted samples were the French rutting tester and the Hamburg wheel-tracking device.

2.1.1 French Rutting Tester

The French rutting tester is used to evaluate the resistance to permanent deformation. It is manufactured by the *Laboratoire Central des Ponts et Chaussees* (LCPC) and is shown in Figure 1: a close-up is shown in Figure 2. The samples tested are 500 x 180 mm (19.7 x 7.1 in.) and can be 50 or 100 mm (2 or 4 in.) thick.

Two samples can be tested simultaneously. The samples are loaded with 5000 N (1124 lbs.) by a pneumatic tire inflated to 0.6 MPa (87 psi). The tires load each sample at 1 cycle per second; one cycle is two passes. The chamber is heated to 60°C (140°F) but can be set to any temperature between 35° and 60°C (95° and 140°F).

When a test is performed on a laboratory compacted sample, it is aged at room temperature for as long as 7 days. It is then placed in the French rutting tester and loaded with 1000 cycles at room temperature. The deformations recorded after the initial loading are the "zero" readings. The sample is then heated to the test temperature for 12 hours before the test begins. Rutting depths are measured after 100, 300, 1000, 3000, 10,000, 30,000 and possibly 100,000 cycles. The rutting depth is reported as a percentage of the sample thickness. After a given number of cycles, the percentage is calculated as the average of 15 measurements (five locations along the length and three along the width) divided by the original slab thickness. A pair of slabs can be tested in about 9 hours.

A successful test will typically have a rutting depth that is less than or equal to 10% of the slab thickness after 30,000 cycles. The results are plotted on a log-log graph paper. The slope and intercept (at 1000 cycles) are calculated using linear regression. The equation is:

Figure 1. French Rutting Tester.

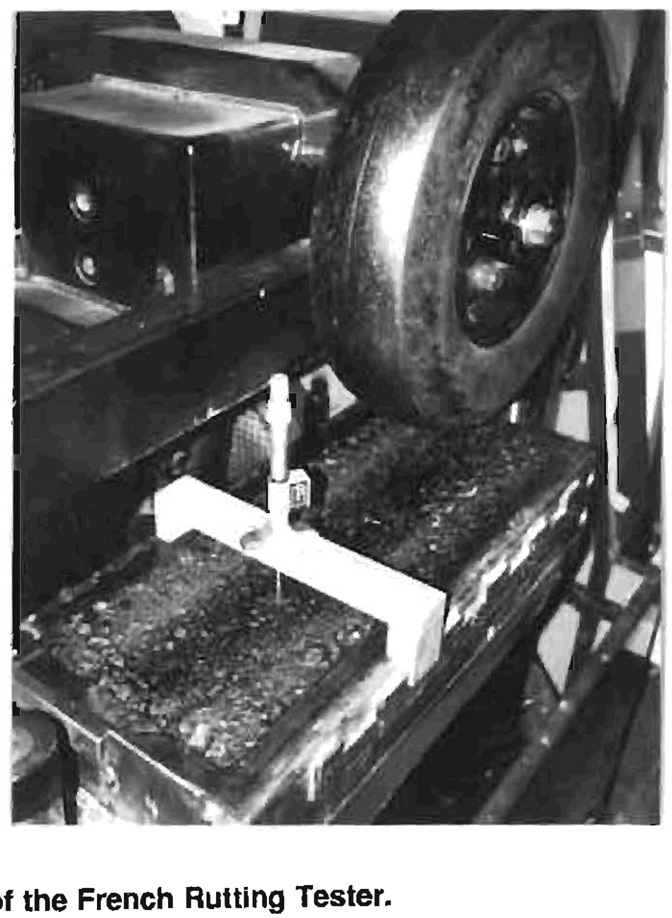

Figure 2. Close-up of the French Rutting Tester.

$$Y = A\left(\frac{X}{1000}\right)^{B} \qquad (Equation\ 1)$$

where:

Y = rutting depth (%),

X = cycles,

A = intercept of the rutting depth at 1000 cycles, and

B = slope of the curve.

2.1.2 Hamburg Wheel-Tracking Device

The Hamburg wheel-tracking device is used to determine the moisture susceptibility of HMA. It is manufactured by Helmut-Wind Inc. of Hamburg, Germany and shown in Fig. 3: a close-up in Fig. 4. A pair of samples are tested simultaneously. A sample is typically 26 cm (10.2 in.) wide, 32 cm (12.6 in.) long, and 40 mm (1.6 in.) deep. Its mass is approximately 7.5 kg (16.5 lbs.), and the sample is compacted to 6 $\pm$ 1% air voids. The samples are submerged under water at 50°C (122°F), although the temperature can vary from 25°C to 70°C (77°F to 158°F). A steel wheel, 47 mm (1.85 in.) wide, loads the samples with 705 N (158 lbs.) The wheel makes 50 passes per minute over each sample. The maximum velocity of the wheel is 34 cm/sec (1.1 ft/sec) in the center of the sample. Each sample is loaded for 20,000 passes or until 20 mm of deformation occur. Approximately 6-1/2 hours are required for a test.

The results from the Hamburg wheel-tracking device include the creep slope, stripping slope and stripping inflection point as shown in Fig. 5. The results have been defined by Hines (2). The creep slope relates to rutting from plastic flow. It is the inverse of the rate of deformation in the linear region of the deformation curve, after post compaction effects have ended and before the onset of stripping. The stripping slope is the inverse of the rate of deformation in the linear region of the deformation curve, after stripping begins and until the end of the test. It is the number of passes required to create a 1 mm impression from stripping. The stripping slope is related to the severity of moisture damage. The stripping inflection point is the number of passes at the intersection of the creep slope and the stripping slope. It is related to the resistance of the HMA to moisture damage.

Figure 3. Hamburg Wheel-Tracking Device.

Figure 4. Close-up of the Hamburg Wheel-Tracking Device.

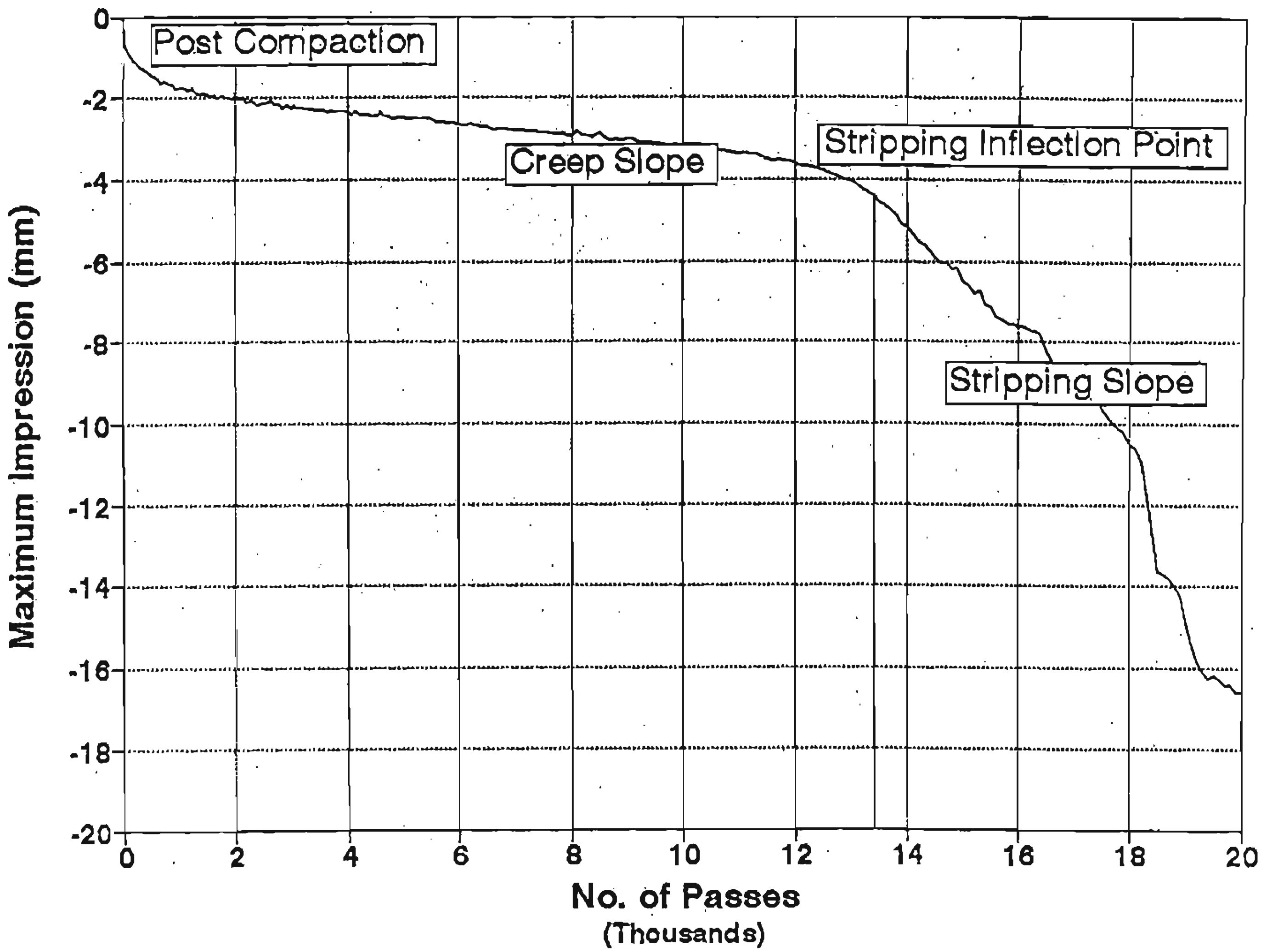

Figure 5. Results from the Hamburg Wheel-Tracking Device.

2.1.3 Air Void Distribution

Since results of the tests are influenced by the air void contents of the samples tested, samples were compacted in the laboratory to an air void content as close to the field compacted sample as possible. Just as differences in the actual air void content of a sample can influence the results, the distribution of air voids throughout the compacted samples could influence the test results. Therefore, samples from each of the compactors and a field compacted sample were sliced into 12 to 24 pieces. The air voids of each piece were measured to determine the distribution of air voids throughout each sample. The distribution of air voids were then compared between the various methods of compaction.

2.2 Laboratory Compactors

The laboratory compactors used to prepare samples for testing include the linear kneading compactor and the French plate compactor.

2.2.1 Linear Kneading Compactor

The linear kneading compactor is shown in Figure 6 and is manufactured by R/H Specialty and Machine in Terre Haute, Indiana. The compactor can produce samples for direct use with both the Hamburg wheel-tracking device and the French rutting tester. Samples 320 x 260 mm (12.6 x 10.2 in.) and 40 mm (1.6 in.) or 80 mm (3.2 in.) thick can be produced on the Hamburg wheel-tracking device. Samples that are 500 mm x 180 mm (19.7 x 7.1 in.) and 50 mm (2 in.) thick can be produced for use on the French rutting tester. Additionally, two lifts of 50 mm can be used to make a 100 mm (4 in.) thick sample for the French rutting tester.

Since samples are compacted to a known height, the targeted air voids of the compacted sample are achieved easily. After determining the maximum specific gravity (AASHTO T 209) of the mix, the mold is filled with a pre-determined weight of material. The sample can then be compacted within $\pm$ 1% of the targeted air voids.

A series of 12-mm (0.5-in.) wide steel plates are placed on the loose mix in the mold. A downward motion of the roller applies a force to the top of each plate while the mold moves back and forth on a sliding table shown in Figure 7. A linear compression wave is produced in the mix by the bottom edges of the plates as the roller pushes down on each plate. This kneading action

Figure 6. Linear Kneading Compactor.

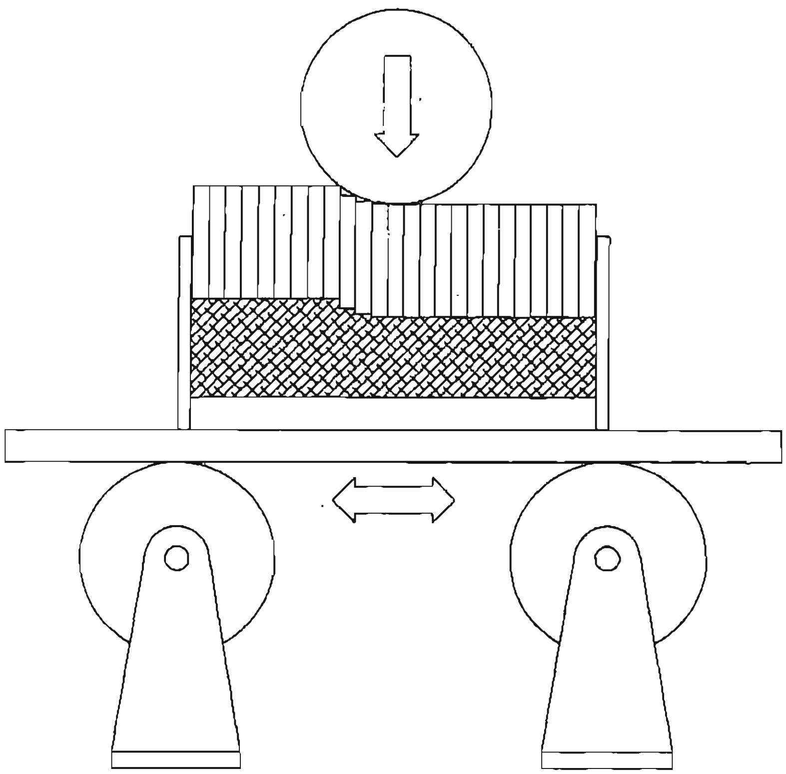

Figure 7. Schematic of the Linear Kneading Compactor.

allows the mix to be compacted without fracturing the aggregate. This compactive action is probably very similar to a steel-wheel roller. The compaction time is less than 10 minutes.

2.2.2 French Plate Compactor

The French plate compactor is shown in Figure 8 and is manufactured in France by the LCPC. Samples compacted are 500 x 180 mm (19.7 x 7.1 in.) and 50 or 100 mm (2 or 4 in.) thick. These samples can be used directly in the French rutting tester. When samples are prepared for the Hamburg wheel-tracking device, the 50 mm thick sample is used and the length is trimmed.

A pneumatic tire is inflated to 0.6 MPa (87 psi). The tire makes 2 passes on each outside edge for every one pass in the center of the sample; for example, the entire sample width can be covered in 5 passes (2 front, 2 back, 1 center), 10 passes (4 front, 4 back, 2 center), 15 passes (6 front, 6 back, 3 center), etc. The force applied by the wheel can vary from 0.2 to 0.6 MPa (29 to 87 psi). Therefore, the compactive effort can be controlled by varying either the number of passes and/or the force applied by the wheel. This compactive effort is very similar to a pneumatic-tired roller. The compaction time is approximately 30 minutes.

As with the linear kneading compactor, a pre-determined weight of material is used based on the maximum specific gravity of the mix. The compaction is stopped when the sample is level with the mold. Since this is a visual determination, it is difficult to precisely control the level of air voids in the sample. Samples can usually be compacted to within ± 2% of the targeted air voids with an experienced operator.

2.3 Experimental Grid

Seven sites were investigated in this study. The testing performed from each site is shown in the experimental grid in Table 1.

Table 1. The Experimental Grid Used for Each Site.

	Compaction Method (Sample Thickness)				
	Field Slab	French (100 mm)	French (50 mm)	Kneading (100 mm)	Kneading (40 mm)
Hamburg Device	X		X		X
French Rutter	X	X	X	X	
Void Distribution	X	X	X		X

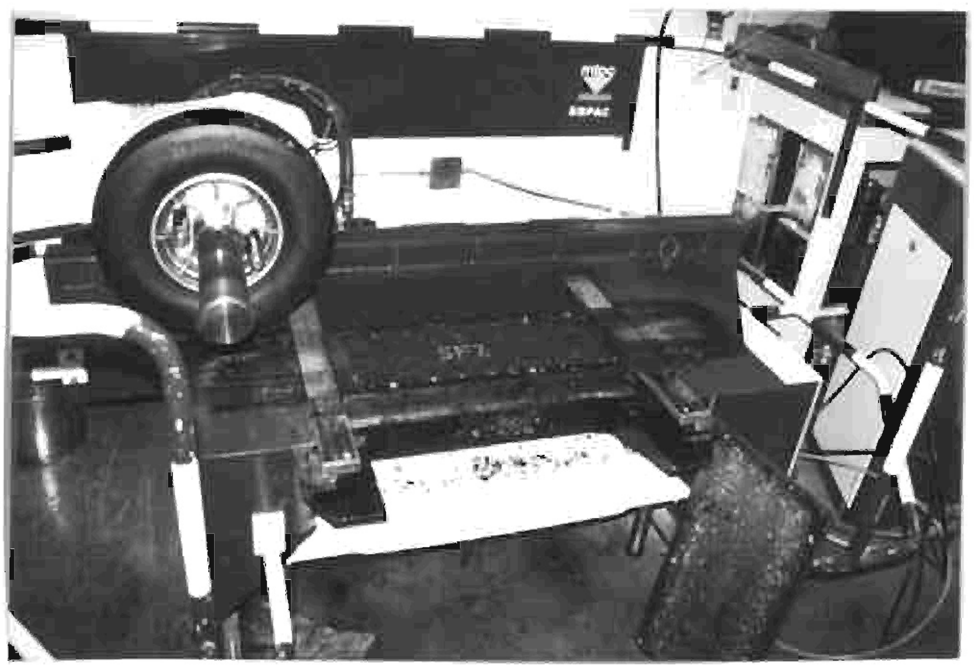

Figure 8. French Plate Compactor.

3.0 Site Information

Seven sites were selected for this study. The following is a brief description of the site location, laydown procedures, and field compaction procedures. A detailed roller pass study from each site is in Appendix A. For the purpose of this study, a pass is defined as one compaction machine rolling back and forth over a selected spot.

A specific location at each site was identified. Loose mix was sampled from this location, and a roller pattern study was performed at this location. The percent relative compaction was measured based on the maximum specific gravity (AASHTO T 209). Field slabs were later sawn and cored at this same location.

3.1 Site 1

Site 1 was located on US-40 just north of Fraser. This project involved the placement of a 50-mm thick overlay using a Grading CX mix. Bottom dump trucks placed the HMA in a windrow, and an elevating loader was used to fill the paver hopper. The loose mix samples were taken from the windrow in front of the paver in the shoulder area of the northbound lane.

The breakdown roller, a HYPAC C766B double-drum vibrating steel wheel roller, made 2.5 passes on this section of pavement. The intermediate roller, a CAT PS-130 pneumatic roller, made 1 pass and the finish roller, a HYPAC C766B steel wheel roller with no vibration, made 2.5 passes to finish the section. The final percent relative compaction achieved at the site was 92%.

3.2 Site 2

Site 2 was located on 120th Avenue between Lamar and Ponderosa Streets in Broomfield. This project involved the placement of a 50-mm thick bottom course using a Grading C mix followed by a 50-mm thick top course using a Grading CX mix. Rear dump trucks placed the HMA into the hopper of a Material Transfer Vehicle (MTV). The MTV then filled the paver hopper. The loose mix samples were taken at the auger of the paver in the outside shoulder area of the eastbound lane during the placement of the bottom course.

The breakdown roller, a CAT double-drum vibrating steel wheel roller, made 1.5 passes on this section of pavement. The intermediate roller, a Hyster C530A pneumatic roller, made 3 passes and the finish roller, a HYPAC C766B double-drum vibrating steel wheel roller, made 5 passes to finish the section. The final percent relative compaction achieved at the site was 93%.

3.3 Site 3

Site 3 was located on Navajo Street, north of Quincy Avenue in Englewood. This project involved the placement of a 50-mm thick overlay using a Grading C mix. Rear dump trucks placed the HMA in the paver hopper. The loose mix samples were taken at the auger of the paver in the southbound lane.

The breakdown roller, a Hyster C766A double-drum vibrating steel wheel roller, made 1.5 passes on this section of pavement. The intermediate roller, a Ferguson FP 912 pneumatic roller, made 4.5 passes and the finish roller, an Ingersoll DA 40 steel wheel roller, made 2 passes to finish the section. The final percent relative compaction achieved at the site was 93%.

3.4 Site 4

Site 4 was located on SH-119 in Boulder Canyon west of Boulder. This project involved the placement of a 32-mm thick overlay using a Grading CX mix. Rear dump trucks placed the HMA in the paver hopper. The loose mix samples were taken at the auger of the paver in the westbound lane.

The breakdown roller, a DYNAPAC CC42 double-drum vibrating steel wheel roller, made 1 pass on this section of pavement. The intermediate roller, a Hyster C530A pneumatic roller, made 6 passes and the finish roller, an Ingersoll DA 40 steel wheel roller, made 1.5 passes to finish the section. The final percent relative compaction achieved at the site was 93%.

3.5 Site 5

Site 5 was located on SH-24, 0.6 miles west of Woodland Park. This project involved the placement of a 50-mm thick overlay using a Grading CX mix. Rear dump trucks placed the HMA in the paver hopper. The loose mix samples were taken at the auger of the paver in the westbound lane.

The breakdown roller, a CAT CD534 double-drum vibrating steel wheel roller, made 1.5 passes on this section of pavement. The intermediate roller, an Ingersoll PT125R pneumatic roller, made 2 passes and the finish roller, a Hyster C350C steel wheel roller, made 0.5 passes to finish the section. The final percent relative compaction achieved at the site was 90%.

3.6 Site 6

Site 6 was located on US-40 near mile post 165 in Muddy Pass north of Kremmling. This project involved the placement of a 50-mm thick overlay using a Grading CX mix. Bottom dump trucks placed the HMA in a windrow, and an elevating loader was used to fill the paver hopper. The loose mix samples were taken from the windrow in front of the paver in the southbound lane.

The breakdown roller, a Hyster C766A double-drum vibrating steel wheel roller, made 1.5 passes on this section of pavement. The intermediate roller, a Hyster C766A double-drum vibrating steel wheel roller that alternated vibrating every 0.5 pass, made 1.5 passes. The finish roller, a Hyster C350C steel wheel roller, made 2.5 passes to finish the section. The final percent relative compaction achieved at the site was 96%.

3.7 Site 7

Site 7 was located on SH-287 in Broomfield. This project involved the placement of a 50-mm thick overlay using a Grading C mix. Rear dump trucks placed the HMA in the paver hopper. The loose mix samples were taken at the auger of the paver in the northbound lane.

The breakdown roller, a DYNAPAC CC42 double-drum vibrating steel wheel roller, made 2 passes on this section of pavement. The intermediate roller, a Hyster C530A pneumatic roller, made 5 passes and the finish roller, a DYNAPAC CC42 double-drum vibrating steel wheel roller, made 2 passes in the static mode to finish the section. The final percent relative compaction achieved at the site was 93%.

4.0 Test Results and Discussion

4.1 Air Void Distribution

Air void distribution throughout the sample might effect the results from testing. The purpose of this testing was to compare the distribution of air voids in laboratory compacted samples with that in the field compacted samples.

To determine the air void distribution, samples from each compactor and from the field were cut into small pieces. For each site a 50-mm thick French, a 40-mm thick linear kneading, and a field compacted sample were cut into 12 pieces each. A 100-mm thick French compacted sample from each site was cut into 24 pieces. Figures 9 and 10 show the actual layout of how the pieces were cut and numbered. Each piece was then measured for air void content according to AASHTO T 166 to determine the distribution. The results from this testing can be seen in Table 2 expressed in terms of the average (avg.) and standard deviation (S.D.)

Table 2. Air Void (%) Distribution - Average and Standard Deviation.

Site	Compactor (Sample Thickness)							
	Field Sample		French (50-mm)		French (100-mm)		Kneading (40-mm)	
	Avg.	S.D.	Avg.	S.D.	Avg.	S.D.	Avg.	S.D.
1	7.6	0.25	7.1	0.47	7.6	1.39	6.8	1.47
2	5.6	0.47	5.6	0.64	6.2	1.22	6.2	1.09
3	7.7	0.15	6.6	0.67	6.8	1.16	5.7	1.01
4	8.4	0.67	7.6	0.68	7.3	1.99	5.9	1.64
5	9.2	0.55	11.4	0.46	7.6	1.17	7.7	1.55
6	5.1	0.54	6.4	0.95	6.3	1.46	3.1	1.30
7	10.7	0.27	9.3	0.98	9.3	1.57	7.3	1.10
Avg.		0.41		0.69		1.42		1.31

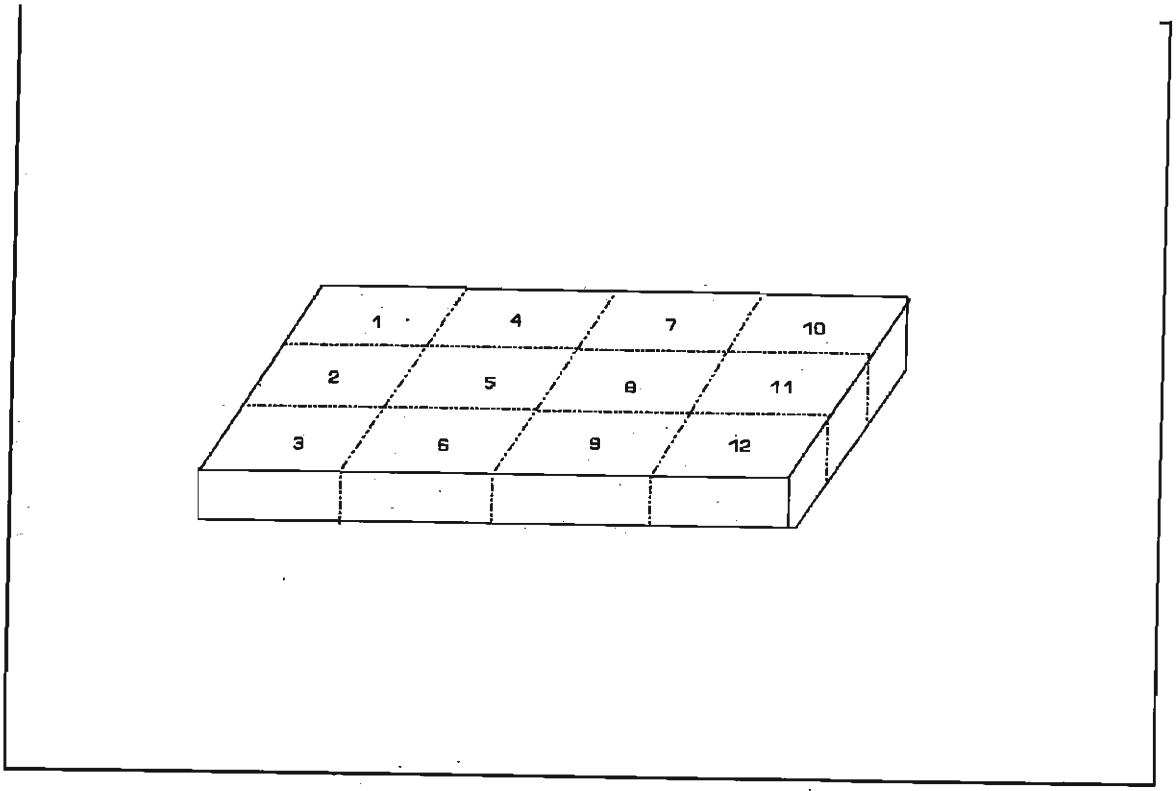

Figure 9. Layout of How 50-mm Thick French, 40-mm Thick Linear Kneading, and Field Compacted Samples Were Cut and Numbered.

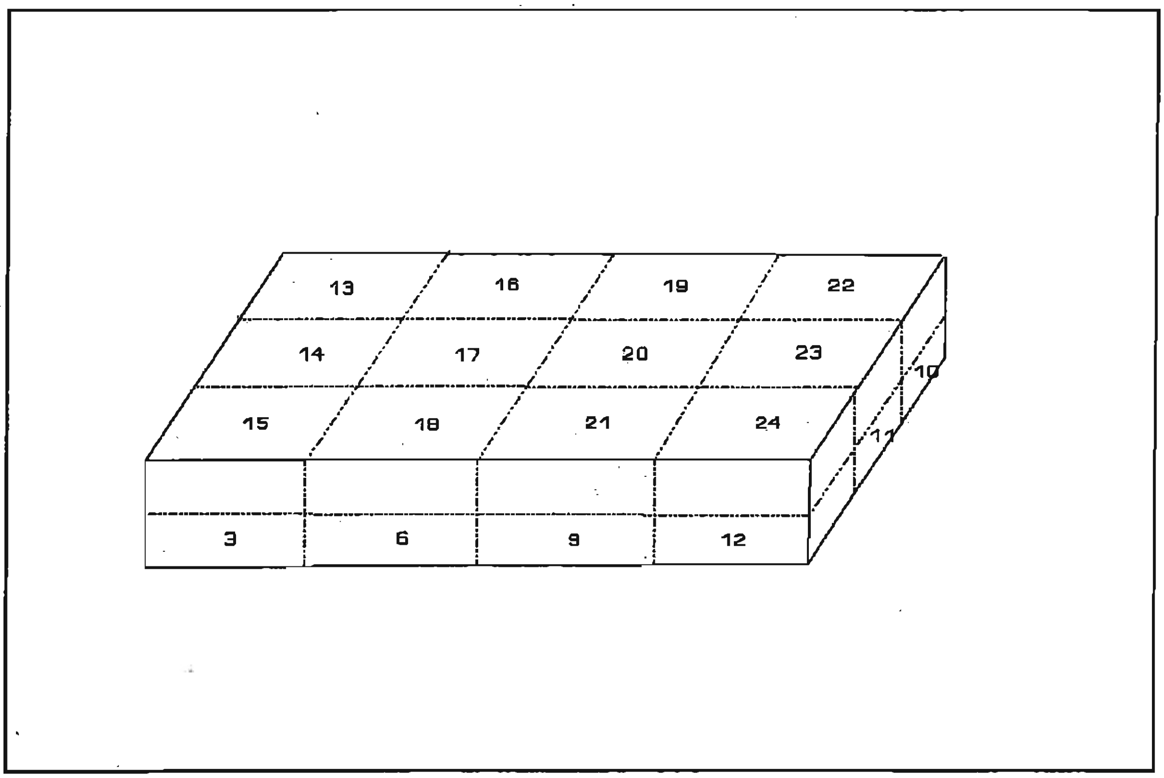

Figure 10. Layout of How 100-mm Thick French Compacted Samples Were Cut and Numbered.

4.1.1 Field Samples

At each site, the air voids were more uniformly distributed in the field compacted samples than in any of the laboratory compacted samples. The small variation of air voids found within the field compacted samples was expected, since they were sawn from the center of the pavement, far from its restrictive corners or edges. The variation in the laboratory compacted samples was due to large deviations at the corners and edges of the sample.

4.1.2 French Compactor

As seen in Table 2, the 100-mm thick French compacted samples have twice as much variation in the distribution of air voids (S.D. of 1.42) as the 50-mm thick French compacted samples (S.D. of 0.69). This difference can be attributed to the thickness of the samples. Table 3 shows the standard deviation of air voids in the top half of the 100-mm thick French compacted samples is 0.62, which is similar to the standard deviation for the complete 50-mm thick French compacted samples (S.D. of 0.69, Table 2) and the 50-mm thick French compacted samples with the corners removed (S.D. of 0.59, Table 3). For each case, the distribution is fairly uniform. The air voids within the bottom half of the 100-mm thick French compacted samples are more variable (S.D. of 1.25, Table 3). This is mainly due to high air voids in its corners (pieces 1, 3, 10, and 12).

The distribution of air voids in a 100-mm thick French compacted sample can be further clarified by observing Figure 11. The entire graph shows a normal distribution skewed towards the higher air voids. The air voids in the top half of the 100-mm thick French compacted sample (pieces 13 through 24) have a uniform and normal distribution. The air voids in the bottom half of the 100-mm thick French compacted sample (pieces 1 through 12) skews the air voids to the high side.

The air voids in the bottom half of the 100-mm thick French compacted samples (S.D. of 1.25) are more dispersed than in the top half (S.D. of 0.62). This is because the air voids in the corners of the bottom half (pieces 1, 3, 10, and 12) are greater than 1 standard deviation from the average percent air void content as shown in Figure 11. Also, for Site 1 the bottom half centers around 8.7% air voids, which is about 2% higher than the average in the top half of 6.6% air voids. The dispersion of air voids throughout the entire sample is increased since the top and bottom halves center around two different values.

Table 3. Air Void (%) Distribution of Portions of Samples.

Site	100-mm French Compacted Samples						50-mm French	
	Top Half		Bottom Half		Bottom w/o Corners		Without Corners	
	Avg.	S.D.	Avg.	S.D.	Avg.	S.D.	Avg.	S.D.
1	6.6	0.29	8.7	1.22	8.0	0.83	7.0	0.39
2	5.5	0.58	7.0	1.20	6.3	0.83	5.4	0.58
3	6.0	0.41	7.7	0.99	7.2	0.78	6.3	0.58
4	5.7	0.95	9.0	1.28	8.3	0.91	7.3	0.67
5	7.5	0.82	7.6	1.44	6.8	0.87	11.3	0.42
6	5.2	0.54	7.3	1.35	6.5	0.75	6.0	0.79
7	8.2	0.72	10.5	1.28	9.8	0.90	8.8	0.72
Avg.		0.62		1.25		0.84		0.59

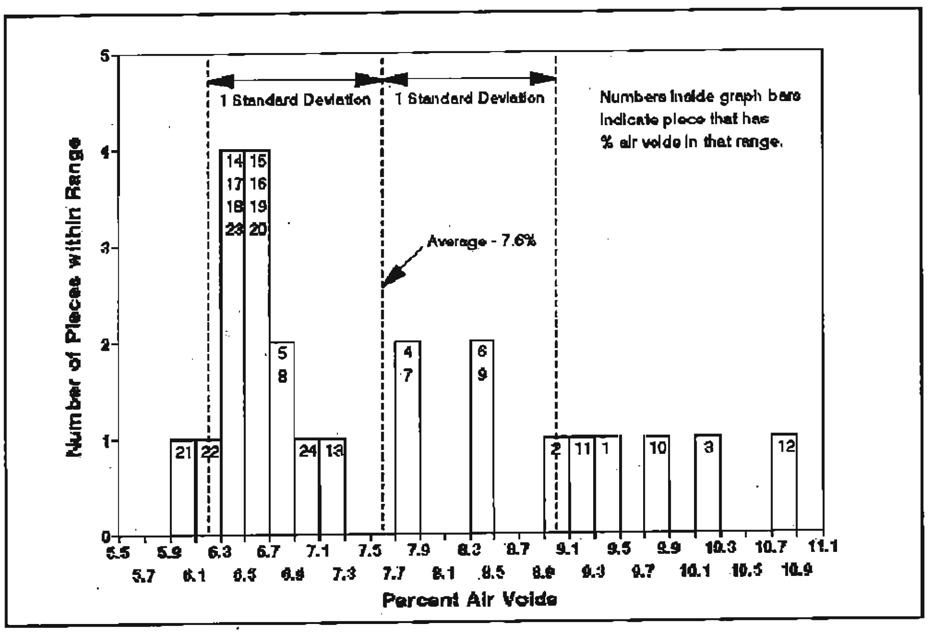

Figure 11. Typical Distribution of Air Voids in a 100-mm Thick French Compacted Sample for Site 1.

In France, the distribution of air voids is checked on each sample with a nuclear device. The air voids are measured at 72 points on the sample, 24 points each on the top, middle, and bottom layers. The standard deviation achieved for a 100-mm thick French compacted sample is typically about 2.0 which is higher than any of the laboratory compacted samples in this study. Thus, the samples in this study are well within the standard deviations obtained by the French. Also, the percent air voids from top to bottom increased 2% in France's sample. As can be seen in Table 3, the 100-mm thick French compacted samples had 2% higher air voids in the bottom half for most sites.

Although there is a fairly uniform distribution in the 50-mm thick French compacted samples, the variability of the distribution of air voids (S.D. of 0.69) is about 1.5 times that of the field compacted samples (S.D. of 0.41). The difference in variability is likely due to the corners and edge pieces of the French compacted samples. The variability in the 100-mm thick French compacted samples (S.D. of 1.42) is about 3 times that of the field samples. This can be attributed to the high variability in the bottom half and corners and edges of the top half as discussed earlier. If the French compactor is used to simulate field compaction, it is recommended that either 1) the 50-mm thick molds be used to compact the samples, or 2) 100-mm thick samples should be compacted in 2 lifts.

4.1.3 Linear Kneading Compactor

As shown in Table 2, the variability of the distribution of air voids in the 40-mm thick linear kneading compacted samples (S.D. of 1.31) is approximately 3 times that of the field compacted samples (S.D. of 0.41). With the linear kneading compactor, it is very important to get the loose mix level in the mold before compacting. Also, extra material is needed in the corners, since they tend to have a higher percentage of air voids. Great care was taken to follow these procedures when compacting the samples for this test.

When the distribution was analyzed, no trend developed as to the cause. The poor distribution was likely caused by not leveling the loose mix in the mold before compacting which is related to operator experience. It was noticed that most of the deviation was from the middle-edge pieces (pieces 4, 6, 7, and 9) of the sample. This was possibly caused by the scraping of material from this area to the corners for extra material. It is recommended that extra material be moved to the corners before leveling of the rest of the material to more evenly distribute the air voids. Also, the development of some type of device to help level the loose material instead of relying on the operators experience might prove to be beneficial.

As seen in Table 2, the variability of air voids in the 40-mm thick linear kneading compacted samples (S.D. of 1.31) is about the same as that of the 100-mm thick French compacted samples (S.D. of 1.42). This, once again, can be attributed to how level the material was before the samples were compacted in the linear kneading compactor. Since the Hamburg wheel-tracking device only passes over the center of the sample where the air void distribution is uniform, results from testing will not be affected by the air voids in the corners or edges. It should be noted that it is much easier to achieve the targeted air void content for the sample with the linear kneading compactor than the French compactor.

4.2 French Rutting Tester

The French rutting tester is used to evaluate resistance to permanent deformation. The purpose of this study is to compare results obtained on the French rutting tester from laboratory compacted samples to those obtained from field compacted samples.

Loose mix was taken at the paver from each site. It was stored in closed containers in the laboratory until time for compacting.

Before the loose mix could be compacted, it needed to be brought to the proper compaction temperature. This compaction temperature varied with the grade of asphalt cement being used at each site. The loose mix was placed in the oven in open containers for about 4 hours. The use of open containers caused additional aging.

The loose mix was then ready to be compacted in the laboratory. For each site, a 50-mm thick sample and a 100-mm thick sample were compacted on the French compactor. Also, a 100-mm thick sample was compacted on the linear kneading compactor. The air voids for samples tested in the French rutting tester are summarized in Appendix B.

For the field compacted samples, a full-depth slab was sawn at each site. These full-depth slabs were approximately 150-mm (6-in.) by 475-mm (19-in.) in size. Only the lift being placed when the loose mix was taken in the field was to be tested. All other lifts were sawn from the samples and discarded. All field compacted samples were plastered into a 50-mm thick mold.

4.2.1 Comparison of Laboratory Compactors.

The samples were placed in the French rutting tester and loaded for 30,000 cycles. Plots of the results are shown in Appendix C. A rutting percentage of greater than 10% of the total thickness of the sample after 30,000 cycles was considered to be a failure. The actual rut depth (R.D.) in millimeter and the rut depth expressed as a percentage of the sample thickness (%) are reported in Table 4.

Table 4. The Rut Depths and Percent Rutting from Samples Tested in the French Rutting Tester.

Site	Compactor (Sample Thickness)							
	French (50-mm)		French (100-mm)		Knead. (100-mm)		Field Slab	
	R.D.	%	R.D.	%	R.D.	%	R.D.	%
1	9.96*	19.15	7.08	7.12	7.70	7.70	4.23	8.08
2	2.50	5.05	5.94	5.91	6.61	6.54	3.61	7.00
3**	3.20	6.70	3.75	3.75	4.00	4.00	19.00	35.70
4	3.28	6.52	4.51	4.56	4.04	4.01	3.82	7.23
5	7.77	16.55	8.78	9.73	6.95	6.93	6.07	11.71
6	1.84	2.74	2.59	2.45	2.30	2.24	0.89	1.76
7	1.78	3.34	2.22	2.49	2.19	2.18	2.35	4.58
Avg.	4.33	8.58	4.98	5.14	4.83	4.80	5.71	10.87

R.D. - Rut depth in millimeters
% - Percent rutting based on initial sample thickness
* Test result at 30,000 cycles was extrapolated from 29,000 cycles.
** Test results are at 20,000 cycles.

As can be seen in Table 4, the actual rut depths of all the samples were fairly similar. The rut depths expressed as a percentage of the sample thickness for the 50-mm thick French compacted samples were 67% higher, on average, of those percentages from the 100-mm thick compacted samples. This difference in percent rut depth would be expected since the 100-mm thick samples are twice the thickness of the 50-mm thick samples.

Table 5 shows that the actual rut depths (R.D.) of the 50-mm thick French compacted samples averaged 0.49 mm less than those from the 100-mm thick linear kneading compacted samples. The actual rut depth of the 100-mm thick French compacted samples average 0.15 mm more than the 100-mm thick linear kneading compacted samples. These difference are very small.

Table 5 also shows that the rut depth expressed as a percentage of the sample thickness (%) for the 50-mm thick French compacted samples averaged 3.94 percent higher than the 100-mm thick linear kneading compacted samples. The percent rut depth for the 100-mm thick French compacted samples averaged only 0.34 percent higher than those of the 100-mm thick linear kneading compacted samples. The large difference between the 50-mm thick samples and the 100-mm thick samples can again be attributed to the 100-mm thick samples being twice the thickness of the 50-mm thick samples.

Table 5. Differences in Rutting Depths Between French and Kneading Compacted Samples.

Site	Compactor (Sample Thickness)			
	French (50-mm) vs. Kneading (100-mm)		French (100-mm) vs. Kneading (100-mm)	
	R.D.	%	R.D.	%
1	2.26	12.61	-0.62	-0.58
2	-4.11	-1.49	-0.67	-0.63
3	-0.80	2.70	-0.25	-0.25
4	-0.76	2.51	0.47	0.55
5	0.82	9.62	1.83	2.80
6	-0.46	0.50	0.29	0.21
7	-0.41	1.16	0.03	0.31
Avg.	-0.49	3.94	0.15	0.34
S.D.	1.939	5.165	0.855	1.173

R.D. - Rut depth in millimeters
% - Percent rutting based on initial sample thickness
Negative numbers indicate a rut measurement was higher in the second sample of the comparison.

4.2.2 Comparison of Laboratory Compactors to Field Compaction.

The field compacted sample at Site 3 failed dramatically while the laboratory compacted samples did not. It is not clear why this happened.

Table 6 shows a comparison of the average difference in actual rut depths (R.D.) and percent rut depths (%) between the laboratory compacted samples and the field compacted samples. The actual rut depths generated by the 50-mm thick French compacted samples averaged 1.03 mm more than those of the field compacted samples. The actual rut depth generated by the 100-mm thick French compacted samples averaged 1.69 mm more than those of the field compacted samples. The actual rut depth generated by the 100-mm thick linear kneading compacted samples averaged 1.47 mm more than the field compacted samples. These average differences are minimal and very similar.

Table 6. Differences in Rutting Depths Between Field and Lab Compacted Samples.

Site	Compactor (Sample Thickness)					
	French (50-mm) vs. Field Slab		French (100-mm) vs. Field Slab		Kneading (100-mm) vs. Field Slab	
	R.D.	%	R.D.	%	R.D.	%
1	5.73	11.07	2.85	-0.96	3.47	-0.38
2	-1.11	-1.95	2.33	-1.09	3.00	-0.46
3*	-15.80	-29.00	-15.25	-31.95	-15.00	-31.70
4	-0.54	-0.53	0.69	-2.67	0.22	-3.22
5	1.70	4.84	2.71	-1.98	0.88	-4.78
6	0.95	0.98	1.70	0.69	1.41	0.48
7	-0.57	-1.24	-0.13	-1.68	-0.16	-2.40
Avg.	1.03	2.20	1.69	-1.28	1.47	-1.79
S.D.	2.54	4.97	1.19	1.15	1.48	2.01

R.D. - Rut depth in millimeters
% - Percent rutting based on initial sample thickness
* - Not included in the averages or standard deviations
Negative numbers indicate a rut measurement was higher in the second sample of the comparison.

Table 6 shows that the rut depth expressed as a percentage of the sample thickness for the 50-mm thick French compacted samples averaged 2.20 percent more than those from the field compacted samples. The percent rut depth from the 100-mm thick compacted samples average 1.5 percent less than those from the field compacted samples. The larger differences from the 100-mm thick samples would again be attributed to them being double the original thickness of the 50-mm thick field compacted samples.

There is very little difference in the actual rut depths from the 50-mm of 100-mm thick samples; however, the percent rut depths in the 50-mm thick samples are different from those of the 100-mm thick samples. Instead of using the percent rut depth, it is recommended to use the actual rut depth for the acceptance criteria.

4.3 Hamburg Wheel-Tracking Device

The Hamburg wheel-tracking device is used to determine the moisture susceptibility of HMA. The purpose of this study was to compare the results obtained from laboratory compacted samples to those results obtained from field compacted samples.

Loose mix was taken at the paver from each site. It was stored in closed containers in the laboratory until compaction time.

Before the loose mix could be compacted, it needed to be brought to the proper compaction temperature. This compaction temperature varied with the grade of asphalt cement being used at each site. The loose mix was placed in the oven in open containers for about 4 hours. The use of open containers caused additional aging.

The loose mix was then ready to be compacted in the laboratory. For each site, two 50-mm thick samples were compacted on the French compactor. These samples were then cut to the proper length to fit in the Hamburg wheel-tracking device molds. Two, 40-mm thick samples were compacted on the linear kneading compactor for each site. The air voids for samples tested in the Hamburg wheel-tracking device are summarized in Appendix B.

For the field compacted samples, two full-depth slabs were sawn at each site. These field compacted samples were approximately 250-mm (10-in.) square. The material to be tested from these field compacted samples was limited to the lift being placed when the loose mix was taken in the field. All other lifts were sawn from the samples and discarded.

An earlier CDOT study (Reference 3) showed that aging affects the results. The difference between field and laboratory aging might affect the comparison of test results from field and laboratory compacted samples. Because of this, additional samples from each site were placed in the oven in closed containers. This minimized the additional aging of the samples. Two 40-mm thick samples from these closed containers were compacted on the linear kneading compactor for each site.

Each pair of slabs was placed in the Hamburg wheel-tracking device and loaded for 20,000 passes of the wheel or until 20 mm of deformation occurred. Plots of the test results are shown in Appendix D. For this study, the stripping inflection points were compared. The resulting stripping inflection points for each pair of samples is shown in Table 7.

Table 7. Stripping Inflection Points (Number of Passes).

Site	Compactor (Sample Thickness)			
	French (50-mm)	Kneading (40-mm)	Field Slab	Kneading (40-mm) Closed Container Aging
1	4600	6900	1000	5000
2	8100	>10,000	3700	9900
3	>10,000	>10,000	4600	7300
4	6900	9500	4300	>10,000
5	>10,000	>10,000	8500	>10,000
6	>10,000	>10,000	>10,000	>10,000
7	>10,000	>10,000	3200	>10,000

In an earlier CDOT study (Reference 4), it was found that any sample with a stripping inflection point greater than 10,000 passes performed well in the field. For this reason, the maximum stripping inflection points recorded in Table 7 was 10,000 passes.

4.3.1 Comparison of Laboratory Compactors.

As can be seen in Table 7, the stripping inflection points were similar for both the 50-mm thick French compacted samples and the 40-mm thick linear kneading compacted samples. There were no stripping inflection points for samples compacted by either method for Sites 3, 5, 6, and 7. For Sites 1, 2, and 4, the stripping inflection points from the samples compacted in the linear kneading compactor were slightly higher than those compacted in the French compactor.

Table 8. Differences in Stripping Inflection Points.

Site	Compactor (Sample Thickness)		
	French (50-mm) vs. Kneading (40-mm)	French (50-mm) vs. Field Slab	Kneading (40-mm) vs. Field Slab
1	-2300	3600	5900
2	-1900	4400	6300
3	0	5400	5400
4	-2600	2600	5200
5	0	1500	1500
6	0	0	0
7	0	6800	6800
Avg.	-971	3471	4443
S.D.	1228	2323	2615

Negative numbers indicate a stripping inflection point was higher in the second sample of the comparison.

Table 8 shows the differences in stripping inflection points between the various samples, the average difference, and the standard deviations. For example, the stripping inflection point for the 50-mm thick French compacted samples from Site 1 (4600 passes) was 2300 passes less than that of the 40-mm thick linear kneading compacted samples (6900 passes). The stripping inflection point for the 50-mm thick French compacted samples from Site 4 (6900 passes) was 2600 passes less than that of the 40-mm thick linear kneading compacted samples (9500 passes).

Overall, the stripping inflection points for the 50-mm thick French compacted samples averaged approximately 1000 passes less than those of the 40-mm thick linear kneading compacted samples. This indicated that there is little influence in the stripping inflection points obtained from samples compacted in the laboratory by either method.

As discussed in section 4.1, the air void distribution of the 50-mm thick French compacted samples was more uniform than that of the 40-mm thick linear kneading compacted sample. This would seem to indicate that the results obtained from the 50-mm thick French compacted samples would differ from those obtained from the 40-mm thick linear kneading compacted samples. The similarity in the stripping inflection points between the two types of laboratory compacted samples shows that this difference in air void distribution between the two compactors is not sufficient to affect the results. Either method of compaction would produce comparable results.

4.3.2 Comparison of Laboratory Compactors to Field Compaction.

Table 7 shows that all field compacted samples did strip and had lower stripping inflection points than any of the laboratory compacted samples. This was likely caused by the laboratory compacted samples having undergone additional aging.

As seen in Table 8, the stripping inflection points for the 50-mm thick French compacted samples averaged 3471 passes more than those obtained from the field compacted samples. The stripping inflection point for the 40-mm thick linear kneading compacted samples averaged 4443 passes (from Table 8) more than those obtained from the field compacted samples. The similarity in these values would once again indicate that both laboratory methods of compaction produce similar results.

4.3.3 Influence of Short-Term Aging

Those laboratory compacted samples brought to compaction temperature in open containers received additional aging. This additional aging might have caused the samples to perform better than those aged in closed containers. For this reason, additional 40-mm thick samples from each sight were brought to compaction temperature in closed containers to minimize additional aging. Table 9 shows the difference in stripping inflection points, the average difference, and the standard deviations when comparing the 40-mm thick linear kneading compacted samples (for both the samples with additional aging and without additional aging) to the field compacted samples.

As can be seen in Table 9, the stripping inflection point for the 40-mm thick linear kneading compacted samples with closed container aging averaged 3843 more than the field compacted samples. The stripping inflection point for the 40-mm thick linear kneading compacted samples with open container aging averaged 4443 passes more than the field compacted samples. The stripping inflection points for the samples with closed container aging were very close to those obtained from the samples with open container aging. Either method of heating the samples to compaction temperature could be used. However, for consistency of results, it is recommended to heat all field samples to compaction temperature in closed containers.

Table 9. Differences In Stripping Inflection Points Between the Kneading Compacted Samples (Both with Additional Aging and with No Additional Aging) and Field Compacted Samples.

Site	Compactor (Sample Thickness)	
	Kneading (40-mm) with Open Container Aging vs. Field Slab	Kneading (40-mm) with Closed Container Aging vs. Field Slab
1	5900	4000
2	6300	6200
3	5400	2700
4	5200	5700
5	1500	1500
6	0	0
7	6800	6800
Avg.	4443	3843
S.D.	2615	2561

It is extremely interesting that laboratory compacted samples perform better than field compacted samples. This should be investigated further. A first hypothesis is that the laboratory compacted samples perform better because of the additional 4 hours of heating (aging) to bring the loose mix to compaction temperature. A second hypothesis is that the laboratory compacted samples are compacted at a much higher temperature (150°C or 300°F) than the field compacted samples (93°C or 200°F).

5.0 Time for Field Compaction

A detailed roller pass study was performed that included temperature measurements is shown in Appendix A. It was decided to compare the actual time it took the mat to cool in the field to the time predicted in the literature.

One of the most important phases of constructing a quality HMA pavement is the field compaction phase. Steel wheel rollers and/or rubber tire rollers are used to reach a percent relative compaction based on the maximum specific gravity (AASHTO T 209). While reaching a specified percent relative compaction is important, it is also important that the pavement is sufficiently hot while compacting. If the pavement is at too low of a temperature, no further compaction will occur and stresses will be placed in the pavement which could potentially cause 1) micro-cracking, 2) broken aggregate, and/or 3) interconnected air voids. For this reason, a minimum compaction temperature is usually specified. There are many opinions on what this minimum temperature should be. The CDOT currently specifies that the percent relative compaction will be reached before the mat surface temperature cools to 85°C (185°F).

It would be beneficial to be able to predict the amount of time it takes a mat to cool to this minimum temperature. This would allow the contractor to know how much equipment is needed at the site to be able to reach the specified percent relative compaction before the mat cools.

In the Hot Mix Asphalt Paving Handbook (5), an article by Dickson (6) is referenced. Reference 6 provides several graphs that can be used to predict the time for a mat to cool. These graphs are based on factors that can affect the rate of cooling. The factors include ambient air temperature, base surface temperature, laydown temperature, mat thickness, wind speed and solar flux. The purpose of this study is to compare the time it takes the mat to cool in the field to the times provided by these graphs.

There are a few problems with using the graphs. Accurately estimating the wind speed and solar flux in the field is difficult. Also, there are an infinite number of combinations of all the factors which affect the rate of cooling. For this reason, the report (6) only provided a few graphs of some common combinations. The problem is that the actual site conditions seldom matched the conditions that the graphs were based on. Also, the report did not remark on how much weight should be given to each factor. This would allow estimating how factors different from the ones that the graphs were based on would change the results obtained from the graphs.

For this study, a surface and an internal (at approximately the center) temperature of the mat in the field were taken with every pass of the roller. The time was recorded when the pavement was initially laid and each time a temperature was measured. From this, the actual time for the mat to cool to a target minimum temperature was obtained. Also, all field conditions that the graphs were based on were recorded. Then these conditions were used along with the graphs to predict a time to cool.

As mentioned earlier, the field conditions were seldom the same as those conditions provided in the graphs. For this reason, graphs with conditions similar but not exact to those conditions of the field were used. In some cases, two graphs were used to get a range of time that the field conditions fell between.

Table 10 shows the actual times for cooling measured in the field and the predicted times for cooling obtained from the graphs. It should be noted that the target minimum temperature for the graphs represented an average temperature throughout the thickness of the mat. There was no mention of where a temperature could be taken in the field to represent this. For this reason, a surface and an internal temperature of the mat were recorded for this study. Later, it was found that Reference 7 stated that a temperature reading of 85°C (185°F) taken 6 mm to 12 mm below the surface of the mat would represent an average mat temperature of 79°C (175°F).

As can be seen in Table 10, the actual field time of cooling in each case was greater than that predicted by the graphs. In most cases it was much greater than that predicted. This is partly due to the differing conditions between the field and the graphs. As mentioned, these times could be compared more accurately (see Appendix A for actual differences in conditions and possible effects of the differences). For this reason, it is assumed that the graphs may underestimate the actual time available for field compaction.

Table 10. Actual and Predicted Times Available to Achieve Field Compaction.

Site	Amount of Time for Mat to Cool to Minimum Compaction Temperature		
	Actual Time (Mat Surface)	Actual Time (Center of Mat)	Predicted Time
1	N/A	50 min.	5-8 min.
2	36 min.	N/A	18-20 min.
3	30 min.	30 min.	16-20 min.
4*	40 min.	10 min.	8-9 min.
5	53 min.	53 min.	9 min.
6	70 min.	70 min.	20 min.
7	40 min.	40 min.	20 min.

N/A - not available.
* - 32-mm thick overlay.

6.0 Conclusions and Recommendations

1) The air void distributions in the field compacted samples were more uniform than those obtained in the laboratory compacted samples. Generally, the results from the tests were not influenced by the differences in distribution of air voids.

2) When using the actual rut depth measured in the French rutting tester, there was very little difference in test results from samples compacted in the various laboratory compactors and field compacted samples. When the percent rutting was measured, the 50-mm thick samples had twice as much percent rutting as the 100-mm thick samples. It is recommended that the actual rut depth be used.

3) When using the Hamburg wheel-tracking device, there was little difference in the stripping inflection point when different laboratory compactors were used. However, field compacted samples typically had much lower stripping inflection points than the laboratory compacted samples. This may be because of either 1) differences in the short-term aging created when the loose field samples are heated to compaction temperature in the laboratory, or 2) the higher compaction temperatures used in the laboratory than in the field.

4) The methods for predicting the available time to achieve field compaction may underestimate the actual time available. The location the temperature is measured can influence the actual time that is believed to be available. Therefore, when specifying the minimum temperatures to achieve field compaction, the location the temperature is measured should also be specified.

7.0 Future Research

It is extremely interesting that laboratory compacted samples perform better than field compacted samples in the Hamburg wheel-tracking device. This should be investigated further. A first hypothesis is that the laboratory compacted samples perform better because of the additional 4 hours of heating (aging) to bring the loose mix to compaction temperature. A second hypothesis is that the laboratory compacted samples are compacted at a much higher temperature (150°C or 300°F) than the field compacted samples (93°C or 200°F). Cores from these sites could be taken when they are one year old to help understand these differences.

8.0 References

1. Report on the 1990 European Asphalt Study Tour (June 1991), American Association of State Highway and Transportation Officials, Washington, D.C., 115+ pages.

2. Hines, Mickey (1991), "The Hamburg Wheel-Tracking Device," Proceedings of the Twenty-Eighth Paving and Transportation Conference, Civil Engineering Department, The University of New Mexico, Albuquerque, New Mexico.

3. Aschenbrener, T, and G. Currier (1993), "Influence of Testing Variables on the Results from the Hamburg Wheel-Tracking Device," Colorado Department of Transportation, CDOT-DTD-R-93-22, 116 pages.

4. Aschenbrener, T., R.L. Terrel, and R.A. Zamora (1994), "Comparison of the Hamburg Wheel-Tracking Device and the Environmental Conditioning System to Pavements of Known Field Performance," Colorado Department of Transportation, CDOT-DTD-R-94-1.

5. Scherocman, J.A. (1991), "Hot-Mix Asphalt Paving Handbook," AASHTO TRB, U.S. Army Corps of Engineers Publication UN-13 (CEMP-ET), 218 pages.

6. Dickson, P.F. and J.S. Corlew (1970), "Thermal Computations Related to the Study of Pavement Compaction Cessation Requirements," Proceedings, Association of Asphalt Paving Technologists, Vol. 39, pp. 377-403.

7. Principles of Construction of Hot-Mix Asphalt Pavements (1983), The Asphalt Institute Manual Series No. 22, Lexington, Kentucky, 291 pages.

Appendix A

Detailed Roller Pass Studies from Each Site

Appendix A
Detailed Roller Pass Studies from Each Site

Roller Pass Study Tables

Note: NP in Number of Passes column indicates that no pass was made by a roller at that time, but a mat temperature reading was taken to help monitor loss of heat. A -Vib. suffix behind the roller type in the Roller column indicates the steel wheel roller was vibrating.

Site 1 - Fraser

PHASE/CODE	MFG./MODEL	TYPE	WT. (kg)	SPEED (kph)
(B) BREAKDOWN	HYPAC C766B	Steel Wheel	8278	3.2
(I) INTERMEDIATE	CAT PS-130	Rubber Tire	3044	12.1
(F) FINISH	HYPAC C766B	Steel Wheel	8278	3.2

Number of Passes	Mat Surface Temp. (Deg. C)	Time	Mat Internal Temp. (Deg. C)	Roller Type/Mode
0.0		1:24	127	B-Vib.
0.5		1:25	127	B-Vib.
1.0		1:25	124	B-Vib.
1.5		1:26	124	B-Vib.
2.0		1:26	124	B-Vib.
2.5		1:27	124	I
3.0		1:28	123	I
3.5		1:30	124	F
NP		1:44	114	
4.0		1:48	111	F
4.5		1:51	109	F
5.0		1:52	108	F
5.5		1:53	107	F
NP		1:55	106	
NP		2:05	99	
NP		2:14	93	

Site 1

FIELD CONDITIONS	
Ambient Air Temperature	15 C
Wind Speed	32.2 Kph
Weather Conditions	Sunny
Mat Thickness	50-mm
Base Surface Temperature	15 C
Laydown Temperature	127 C
Time for Mat Surface Temperature to Cool to 93 C	N/A
Time for Mat Internal Temperature to Cool to 93 C	50 min.

GRAPH CONDITIONS	
Ambient Air Temperature	16 C
Base Surface Temperature	16 C
Laydown Temperature	121 C
Mat Thickness	50-mm
Wind Speed	37 Kph
Weather Conditions	Sunny
Time for Mat to Cool to 93 C	5 min.

GRAPH CONDITIONS	
Ambient Air Temperature	16 C
Base Surface Temperature	16 C
Laydown Temperature	135 C
Mat Thickness	50-mm
Wind Speed	37 Kph
Weather Conditions	Sunny
Time for Mat to Cool to 93 C	8 min.

Our laydown temperature (127 C) falls between the graphs' 121 C and 135 C. With all other conditions being similar, the time for cooling given by the graphs in this case would be somewhere between 5 and 8 minutes. The actual time of 50 minutes shows the graph being very conservative for this site.

Note: No surface temperatures were taken at site 1 because heat spy gun was not available.

Roller Pass Study Tables

Site 2 - 120th Street in Broomfield

PHASE/CODE	MFG./MODEL	TYPE	WT. (kg)	SPEED (kph)
(B) BREAKDOWN	CAT	Steel Wheel	9117	5.6
(I) INTERMEDIATE	Hyster C530A	Rubber Tire	10886	5.6
(F) FINISH	HYPAC C766B	Steel Wheel	8618	5.6

Number of Passes	Mat Surface Temp. (Deg. C)	Time	Mat Internal Temp. (Deg. C)	Roller Type/Mode
0.0		9:20		B-Vib.
0.5		9:40		B-Vib.
1.0		9:41		B-Vib.
1.5		9:43		I
2.0	121	9:44		I
2.5		9:45		I
3.0	118	9:46		I
3.5	118	9:46		I
NP	111	9:49		
NP	110	9:50		
4.0	104	9:51		I
4.5	93	9:52		I
5.0	82	9:56		F-Vib.
5.5	77	9:57		F-Vib.
6.0	77	9:57		F-Vib.
6.5	76	9:59		F-Vib.
7.0	75	10:00		F-Vib.
7.5	72	10:01		F-Vib.
8.0	67	10:02		F-Vib.
8.5	57	10:21		F-Vib.
9.0	54	10:24		F-Vib.
9.5	52	10:25		F-Vib.

Note: No internal temperatures were taken at site 2 because the thermometer malfuntioned.

Site 2

FIELD CONDITIONS	
Ambient Air Temperature	11 C
Wind Speed	8 Kph
Weather Conditions	Night Time
Mat Thickness	50-mm
Base Surface Temperature	13 C
Laydown Temperature	154 C
Time for Mat Surface Temperature to Cool to 49 C	36 min.
Time for Mat Internal Temperature to Cool to 49 C	N/A

GRAPH CONDITIONS	
Ambient Air Temperature	16 C
Base Surface Temperature	16 C
Laydown Temperature	149 C
Mat Thickness	50-mm
Wind Speed	19 Kph
Weather Conditions	Sunny
Time for Mat to Cool to 49 C	20 min.

GRAPH CONDITIONS	
Ambient Air Temperature	10 C
Base Surface Temperature	10 C
Laydown Temperature	149 C
Mat Thickness	50-mm
Wind Speed	19 Kph
Weather Conditions	Sunny
Time for Mat to Cool to 49 C	18 min.

For this site, the graphs show the mat cooling to 79 C in 18 to 20 minutes. Our actual time to cool to this temperature was 36 minutes. The wind speed at this site was less than half of the wind speed the graphs were based on. This would slow the rate of field cooling. Also, this was a night job. The lack of solar flux would decrease the rate of field cooling. When these differing conditions are taken into account, the graph might be close to the actual time.

Roller Pass Study Tables

Site 3 - Navaho Street in

PHASE/CODE	MFG./MODEL	TYPE	WT. (kg)	SPEED (kph)
(B) BREAKDOWN	Hyster C766A	Steel Wheel	9625	4.0
(I) INTERMEDIATE	Ferg. FP912	Rubber Tire	4037	9.7
(F) FINISH	Inger. DA40	Steel Wheel	6994	3.2

Number of Passes	Mat Surface Temp. (Deg. C)	Time	Mat Internal Temp. (Deg. C)	Roller Type/Mode
0.0	143	9:13	143	
NP	131	9:18	110	
0.5	131	9:19	107	B-Vib.
1.0	119	9:22	111	B-Vib.
NP	116	9:25	106	
NP	108	9:30	96	
1.5	91	9:35	87	B-Vib.
2.0	90	9:36	83	I
2.5	89	9:39	82	I
3.0	89	9:39	82	I
3.5	89	9:40		I
4.0	89	9:40		I
4.5	85	9:41		I
5.0	85	9:41		I
5.5	82	9:42		I
6.0	79	9:43	72	I
NP	75	9:45	71	
NP	73	9:50	70	
6.5	66	9:57	66	F-Vib.
7.0	66	9:58	63	F-Vib.
7.5	56	10:01	61	F-Vib.
8.0	52	10:08	54	F-Vib.

Note: No internal temperatures were taken for passes 3.5 through 5.5 at site 3 so that damage to the thermometer probe could be prevented when roller passed over area.

Site 3

FIELD CONDITIONS	
Ambient Air Temperature	16 C
Wind Speed	8 Kph
Weather Conditions	Sunny
Mat Thickness	50-mm
Base Surface Temperature	16 C
Laydown Temperature	143 C
Time for Mat Surface Temperature to Cool to 49 C	30 min.
Time for Mat Internal Temperature to Cool to 49 C	30 min.

GRAPH CONDITIONS	
Ambient Air Temperature	16 C
Base Surface Temperature	16 C
Laydown Temperature	149 C
Mat Thickness	50-mm
Wind Speed	19 Kph
Weather Conditions	Sunny
Time for Mat to Cool to 49 C	20 min.

GRAPH CONDITIONS	
Ambient Air Temperature	16 C
Base Surface Temperature	16 C
Laydown Temperature	135 C
Mat Thickness	50-mm
Wind Speed	19 Kph
Weather Conditions	Sunny
Time for Mat to Cool to 49 C	16 min.

For this site, the graph shows the mat cooling to 79 C in 16 to 20 minutes. Our actual time to cool to this temperature was 30 minutes. The wind speed at this site was less than half of the wind speed that the graph was based on. This would slow the rate of field cooling. When this differing condition is taken into account, the graph might be close to the actual time.

Roller Pass Study Tables

Site 4 - Boulder Canyon

PHASE/CODE	MFG./MODEL	TYPE	WT. (kg)	SPEED (kph)
(B) BREAKDOWN	DYNAPAC CC42	Steel Wheel	10886	3.2
(I) INTERMEDIATE	Hyster C530A	Rubber Tire	10886	12.1
(F) FINISH	Dresser D712	Steel Wheel	8165	3.2

Number of Passes	Mat Surface Temp. (Deg. C)	Time	Mat Internal Temp. (Deg. C)	Roller Type/Mode
0.0	156	9:00	156	
0.5	151	9:10	75	B-Vib.
1.0	143	9:13	74	B-Vib.
1.5	126	9:20	67	I
2.0	124	9:21	67	I
2.5	117	9:22	65	I
3.0	115	9:22	64	I
3.5	109	9:23	63	I
4.0	98	9:26	60	I
4.5	95	9:27	59	I
5.0	92	9:27	58	I
5.5	89	9:29	57	I
6.0	88	9:29	57	I
6.5	84	9:30	56	I
7.0	85	9:30	56	I
NP	59	9:45	44	
7.5	61	9:49	42	F
8.0	68	9:52	41	F
8.5	64	9:52	41	F

Site 4

FIELD CONDITIONS	
Ambient Air Temperature	10 C
Wind Speed	3 Kph
Weather Conditions	Sunny
Mat Thickness	32-mm
Base Surface Temperature	2 C
Laydown Temperature	156 C
Time for Mat Surface Temperature to Cool to 49 C	40 min.
Time for Mat Internal Temperature to Cool to 49 C	10 min.

GRAPH CONDITIONS	
Ambient Air Temperature	-1 C
Base Surface Temperature	-1 C
Laydown Temperature	149 C
Mat Thickness	32-mm
Wind Speed	19 Kph
Weather Conditions	Sunny
Time for Mat to Cool to 49 C	8 min.

GRAPH CONDITIONS	
Ambient Air Temperature	4 C
Base Surface Temperature	4 C
Laydown Temperature	149 C
Mat Thickness	32-mm
Wind Speed	19 Kph
Weather Conditions	Sunny
Time for Mat to Cool to 49 C	9 min.

For this site, the graph shows the mat cooling to 79 C in 8 to 9 minutes. Our actual time to cool to this temperature was 10 minutes. The wind speed at this site was much lower than the graphs' wind speed. This would slow the rate of field cooling. Also, the ambient air temperature at this site was higher than that used in the graphs. This would slow the rate of field cooling. Our laydown temperature was higher than the graphs'. This would allow more time for compaction. When these differing conditions are taken into account, the graph might be close to the actual time.

Roller Pass Study Tables

Site 5 - Woodland Park

PHASE/CODE	MFG./MODEL	TYPE	WT. (kg)	SPEED (kph)
(B) BREAKDOWN	CAT CD534	Steel Wheel	9117	4.8
(I) INTERMEDIATE	Inger. PT125R	Rubber Tire	4620	8.0
(F) FINISH	Hyster C530C	Steel Wheel	7257	4.8

Number of Passes	Mat Surface Temp. (Deg. C)	Time	Mat Internal Temp. (Deg. C)	Roller Type/Mode
0.0	154	9:52	154	
NP	149	9:55		
0.5	119	9:58	139	B-Vib.
1.0	118	10:05	139	B-Vib.
1.5	102	10:13	102	B-Vib.
2.0	102	10:18	96	I
2.5	101	10:19	96	I
3.0	100	10:20	95	I
3.5	100	10:20	94	I
NP	85	10:30	84	
NP	79	10:45	71	
4.0	71	10:51	67	F
NP	64	11:00	62	

Site 5

FIELD CONDITIONS	
Ambient Air Temperature	7 C
Wind Speed	3 Kph
Weather Conditions	Cloudy
Mat Thickness	50-mm
Base Surface Temperature	-1 C
Laydown Temperature	68 C
Time for Mat Surface Temperature to Cool to 79 C	53 min.
Time for Mat Internal Temperature to Cool to 79 C	53 min.

GRAPH CONDITIONS	
Ambient Air Temperature	-1 C
Base Surface Temperature	-1 C
Laydown Temperature	65 C
Mat Thickness	50-mm
Wind Speed	19 Kph
Weather Conditions	Sunny
Time for Mat to Cool to 79 C	9 min.

For this site, the graph shows the mat cooling to 79 C in 9 minutes. Our actual time to cool to this temperature was 53 minutes. The wind speed at this site was much lower than the graphs' wind speed. This would slow the rate of field cooling. Also, the ambient air temperature at this site was higher than that used in the graph. This would also slow the rate of field cooling. Our laydown temperature was higher than the graphs'. This would increase the time available for compaction. When these differing conditions are taken into account, the graph might be conservative at this site.

Roller Pass Study Tables

Site 6 - Muddy Pass

PHASE/CODE	MFG./MODEL	TYPE	WT. (kg)	SPEED (kph)
(B) BREAKDOWN	Hyster C766A	Steel Wheel	8278	4.0
(I) INTERMEDIATE	Hyster C766A	Steel Wheel	8278	4.0
(F) FINISH	Hyster C350C	Steel Wheel	7257	4.8

Number of Passes	Mat Surface Temp. (Deg. C)	Time	Mat Internal Temp. (Deg. C)	Roller Type/Mode
0.0	185	10:30	185	
0.5	110	11:12		B-Vib.
1.0	104	11:15		B-Vib.
1.5	93	11:16	118	B-Vib.
NP	104	11:20	107	
NP	104	11:25	97	
NP	87	11:30	87	
2.0	84	11:33	85	I-Vib.
2.5	83	11:34	84	I
NP	71	11:45	71	
3.0		11:51	66	I-Vib.
3.5	53	12:07	56	F
4.0	53	12:08	56	F
4.5		12:13		F
5.0		12:14		F
5.5		12:15	52	F

Site 6

FIELD CONDITIONS	
Ambient Air Temperature	15 C
Wind Speed	8 Kph
Weather Conditions	Sunny
Mat Thickness	50-mm
Base Surface Temperature	16 C
Laydown Temperature	185 C
Time for Mat Surface Temperature to Cool to 79 C	70 min.
Time for Mat Internal Temperature to Cool to 79 C	70 min.

GRAPH CONDITIONS	
Ambient Air Temperature	16 C
Base Surface Temperature	16 C
Laydown Temperature	149 C
Mat Thickness	50-mm
Wind Speed	19 Kph
Weather Conditions	Sunny
Time for Mat to Cool to 79 C	20 min.

For this site, the graph shows the mat cooling to 79 C in 20 minutes. Our actual time to cool to this temperature was 70 minutes. The wind speed at this site was much lower than the graph's wind speed. This would slow the rate of field cooling. Our laydown temperature was much higher than the graph's. This would increase the time available for compaction. When these differing conditions are taken into account, the graph might be slightly conservative at this site.

Roller Pass Study Tables

Site 7 - SH287 in Broomfield

PHASE/CODE	MFG./MODEL	TYPE	WT. (kg)	SPEED (kph)
(B) BREAKDOWN	DYNAPAC CC42	Steel Wheel	10886	4.0
(I) INTERMEDIATE	Hyster C530A	Rubber Tire	10886	11.3
(F) FINISH	DYNAPAC CC42	Steel Wheel	10886	4.0

Number of Passes	Mat Surface Temp. (Deg. C)	Time	Mat Internal Temp. (Deg. C)	Roller Type/Mode
0.0	168	9:45	168	
NP	141	10:00	138	
NP	141	10:05	124	
0.5	110	10:09	117	B-Vib.
1.0	110	10:13	109	B-Vib.
1.5	103	10:15	107	B-Vib.
2.0	103	10:16	103	B-Vib.
NP	91	10:25	91	
2.5		10:27		I
3.0		10:29		I
3.5		10:32		I
4.0		10:33		I
4.5		10:35		I
5.0	69	10:38		I
5.5	69	10:45		I
6.0	67	10:46		I
6.5	67	10:46		I
7.0	64	10:48		I
7.5	59	11:03		F
8.0	59	11:04		F
8.5	59	11:04		F
9.0	55	11:05		F

Site 7

FIELD CONDITIONS	
Ambient Air Temperature	23 C
Wind Speed	3 Kph
Weather Conditions	Sunny
Mat Thickness	50-mm
Base Surface Temperature	27 C
Laydown Temperature	168 C
Time for Mat Surface Temperature to Cool to 79 C	40 min.
Time for Mat Internal Temperature to Cool to 79 C	40 min.

GRAPH CONDITIONS	
Ambient Air Temperature	16 C
Base Surface Temperature	16 C
Laydown Temperature	65 C
Mat Thickness	50-mm
Wind Speed	19 Kph
Weather Conditions	Sunny
Time for Mat to Cool to 79 C	20 min.

For this site, the graph shows the mat cooling to 79 C in 20 minutes. Our actual time to cool to this temperature was 40 minutes. The wind speed at this site was much lower than the graphs' wind speed. This would slow the rate of field cooling. Our laydown temperature was much higher than the graph's. This would increase the time available for compaction. Also, our base and ambient air temperature are much higher than those of the graph. This would increase the time available for compaction. When these differing conditions are taken into account, the graph might be slightly conservative at this site.

Appendix B

Air Voids of Compacted Samples

Appendix B
Air Voids of Compacted Samples

French Rutter % Air Voids Table

Site	Target Voids	Compactor			
		French (50 mm)	French (100 mm)	Kneading (100 mm)	Field Slab
1	8.0%	7.1%	7.7%	7.6%	8.2%
2	7.0%	6.6%	7.5%	6.6%	8.0%
3	7.0%	6.7%	7.0%	7.4%	7.9%
4	7.0%	6.4%	7.1%	6.9%	8.5%
5	10.0%	11.5%	11.3%	9.8%	9.3%
6	4.0%	5.7%	6.2%	5.1%	4.2%
7	7.0%	9.5%	9.0%	7.6%	10.2%

Hamburg % Air Voids Table

Site	Target Voids	Compactor							
		French (50 mm)		Kneading (40 mm)		Field Slab		Kneading Not Aged	
		A	B	A	B	A	B	A	B
1	8.0%	7.8%	7.2%	7.7%	7.8%	8.5%	8.3%	7.4%	7.8%
2	7.0%	7.1%	6.9%	7.1%	6.6%	8.4%	7.3%	6.9%	7.0%
3	7.0%	7.0%	7.0%	6.9%	6.4%	7.9%	8.0%	6.4%	6.9%
4	7.0%	6.7%	7.2%	6.5%	6.5%	8.2%	8.2%	6.6%	N/A
5	10.0%	11.4%	8.6%	9.8%	9.7%	8.5%	9.0%	9.7%	9.2%
6	4.0%	5.2%	5.7%	5.3%	4.2%	4.1%	4.4%	4.5%	4.2%
7	7.0%	9.4%	9.0%	7.1%	7.2%	10.3%	10.5%	7.5%	N/A

Appendix C

French Rutting Tester Results

SITE 1, 50-mm Thick French Sample

Actual Rut Depth

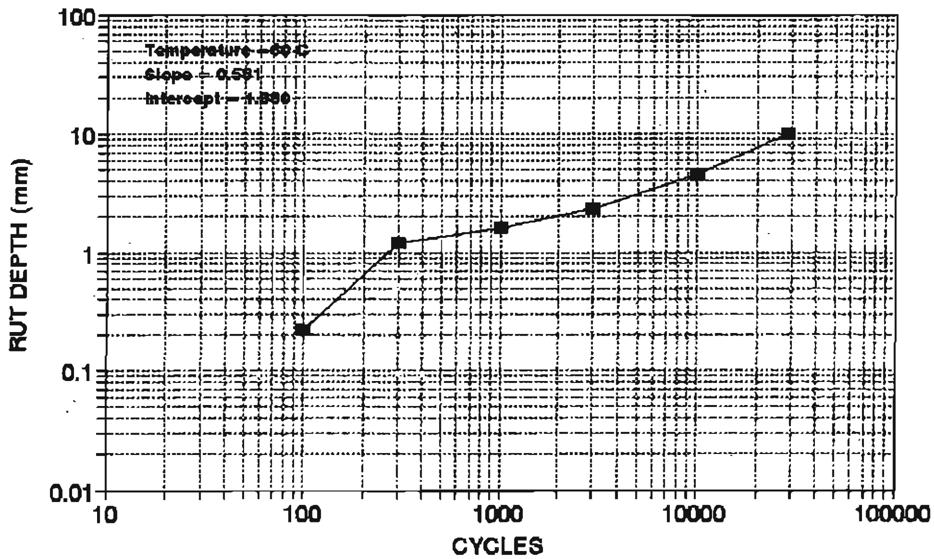

SITE 1, 100-mm Thick French Sample

Actual Rut Depth

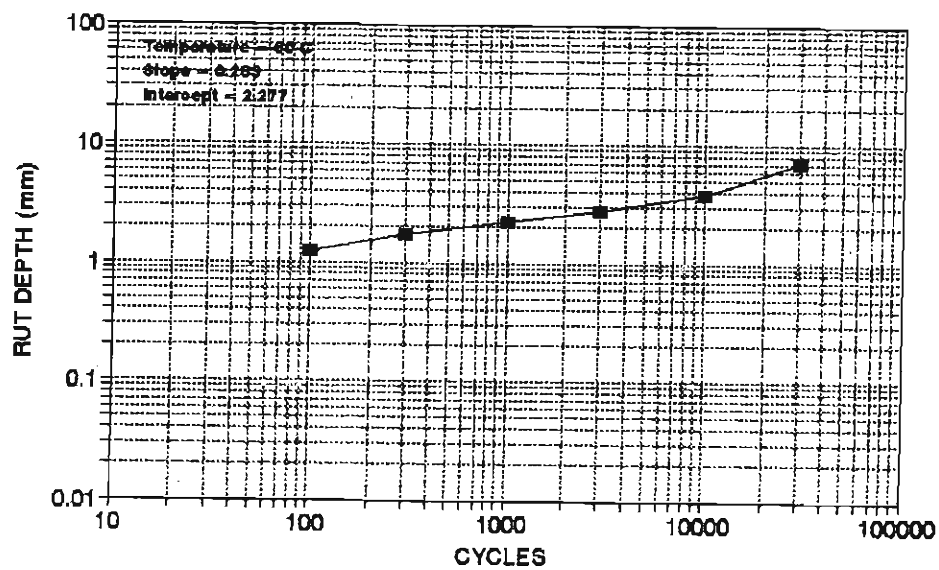

SITE 1, 100-mm Thick Linear Kneading

Actual Rut Depth

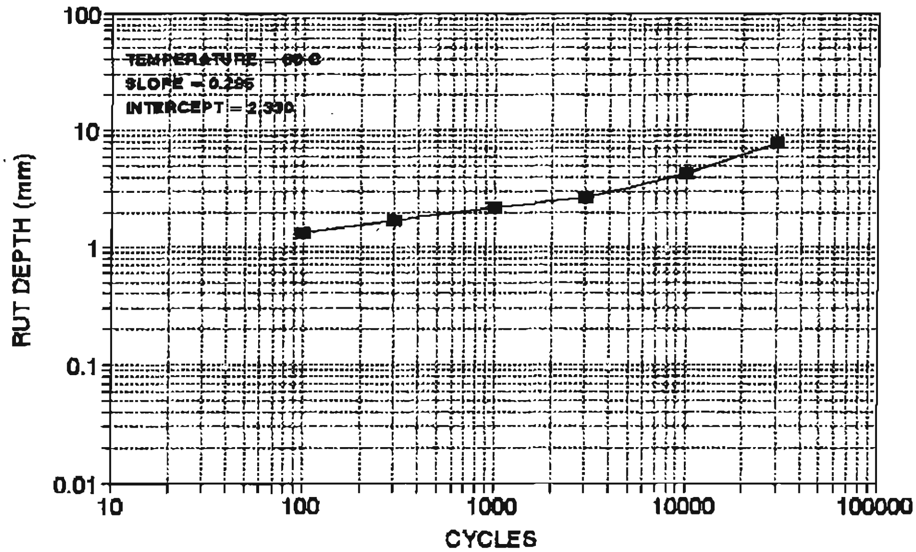

SITE 1, 50-mm Thick Field Sample

Actual Rut Depth

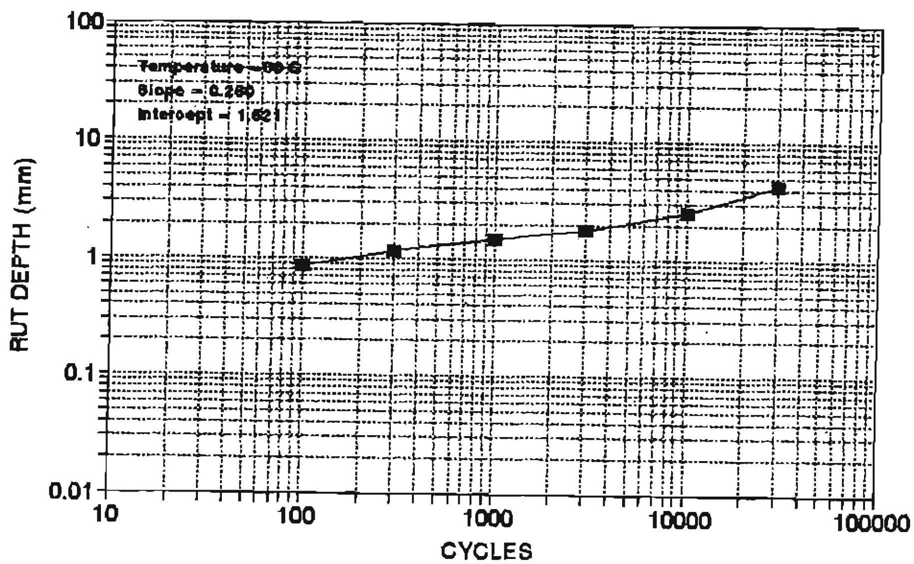

SITE 2, 50-mm Thick French Sample

Actual Rut Depth

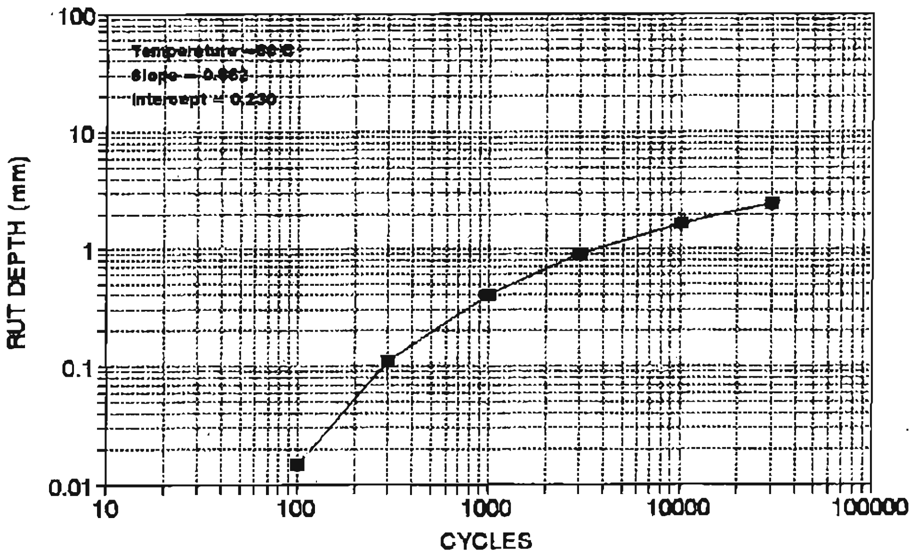

SITE 2, 100-mm Thick French Sample

Actual Rut Depth

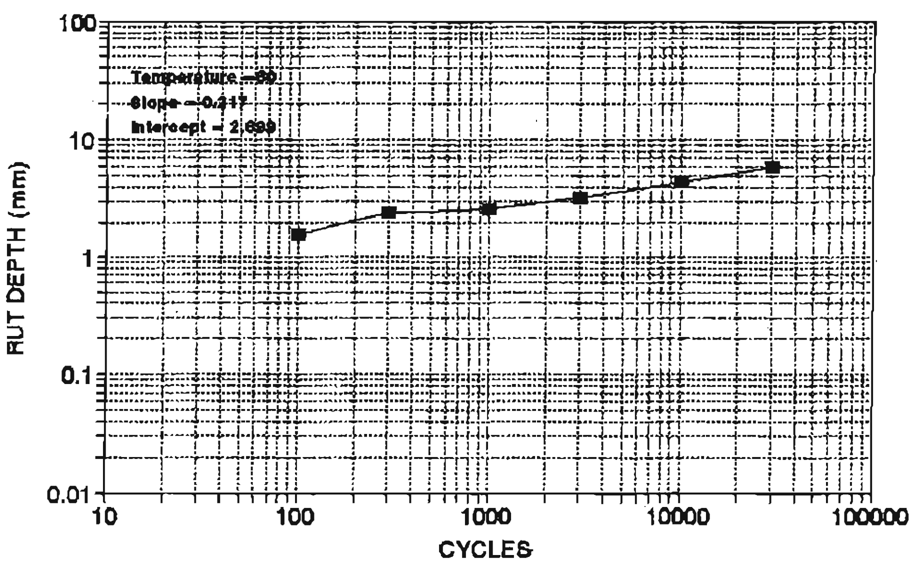

SITE 2, 100-mm Thick Linear Kneading

Actual Rut Depth

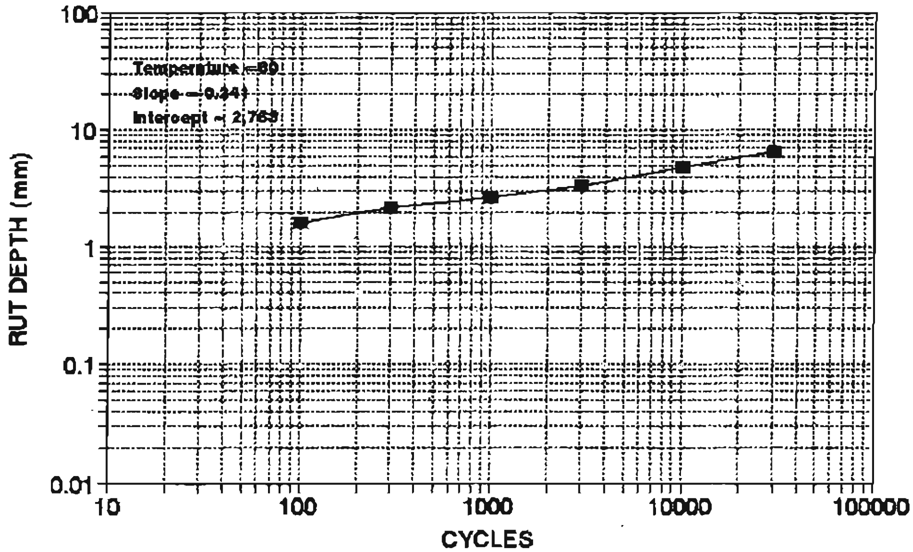

SITE 2, 50-mm Thick Field Sample

Actual Rut Depth

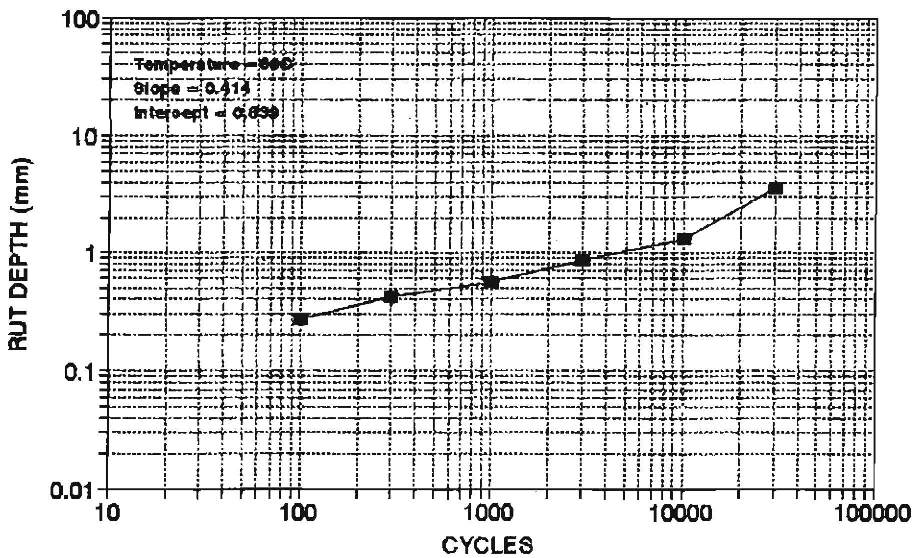

SITE 3, 50-mm Thick French Sample

Actual Rut Depth

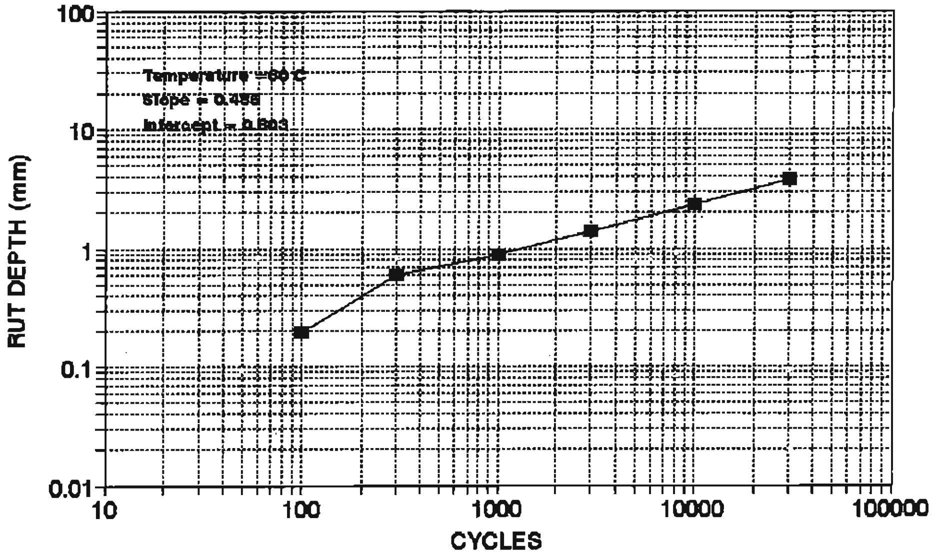

SITE 3, 100-mm Thick French Sample

Actual Rut Depth

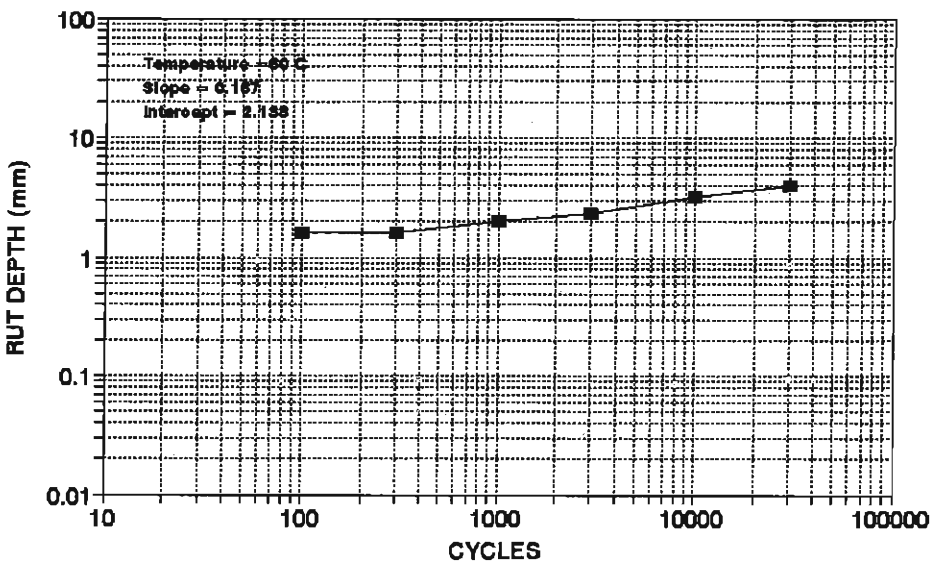

SITE 3, 100-mm Thick Linear Kneading

Actual Rut Depth

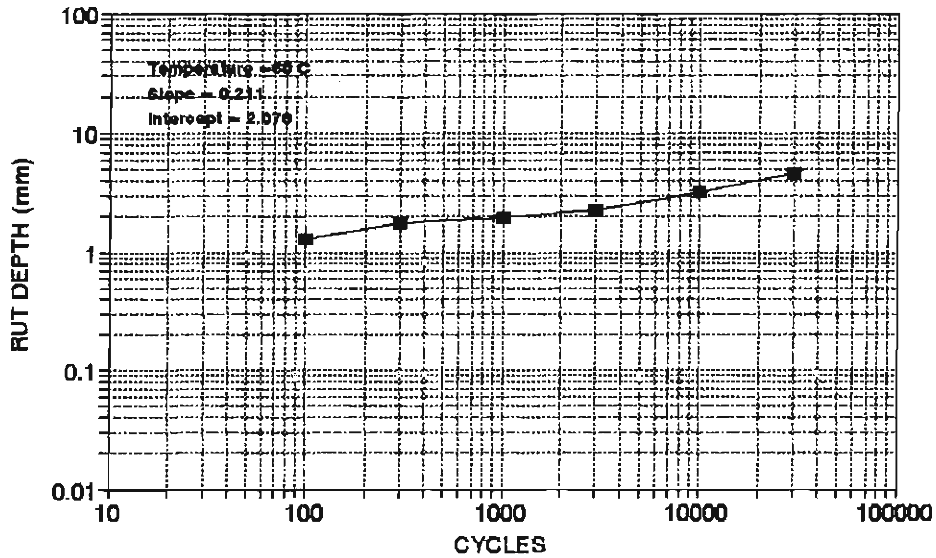

SITE 3, 50-mm Thick Field Sample

Actual Rut Depth

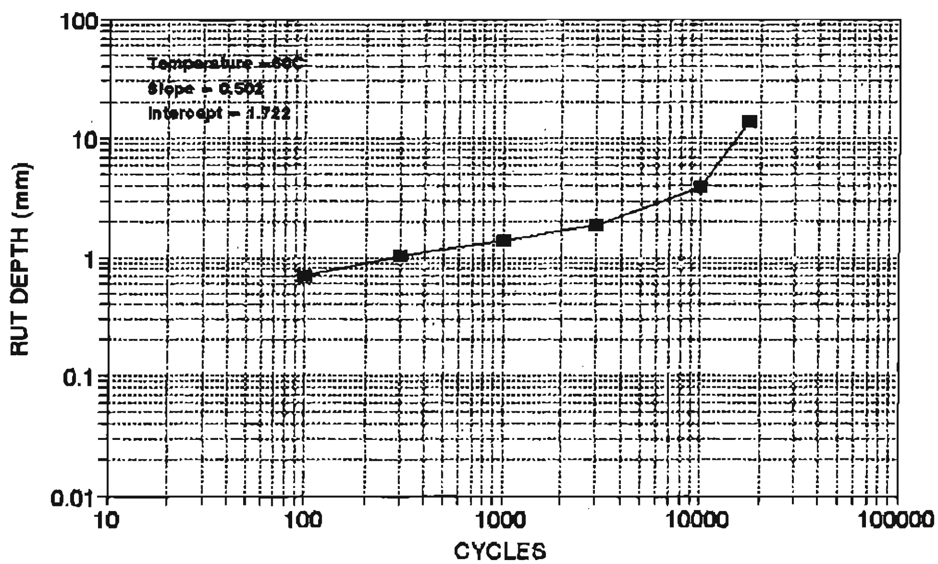

SITE 4, 50-mm Thick French Sample

Actual Rut Depth

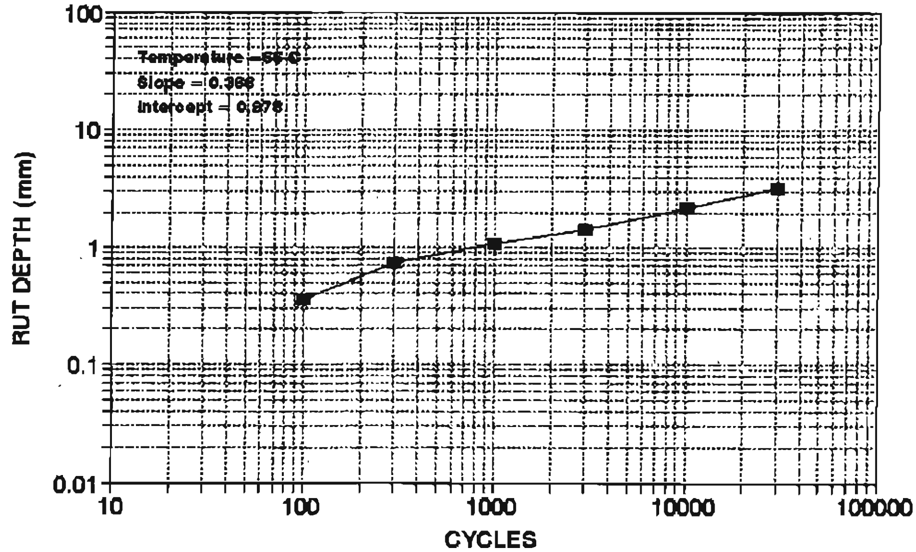

Site 4, 100-mm Thick French Sample

Actual Rut Depth

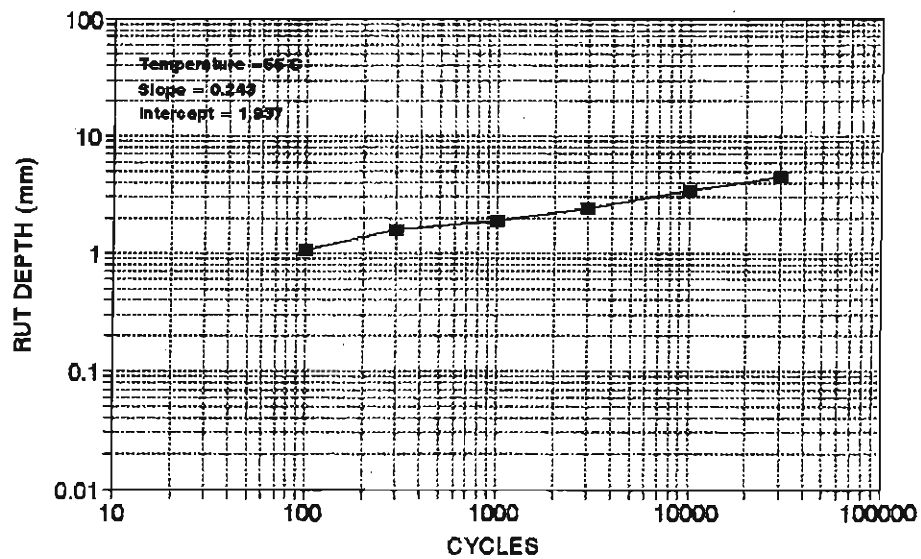

Site 4, 100-mm Thick Linear Kneading

Actual Rut Depth

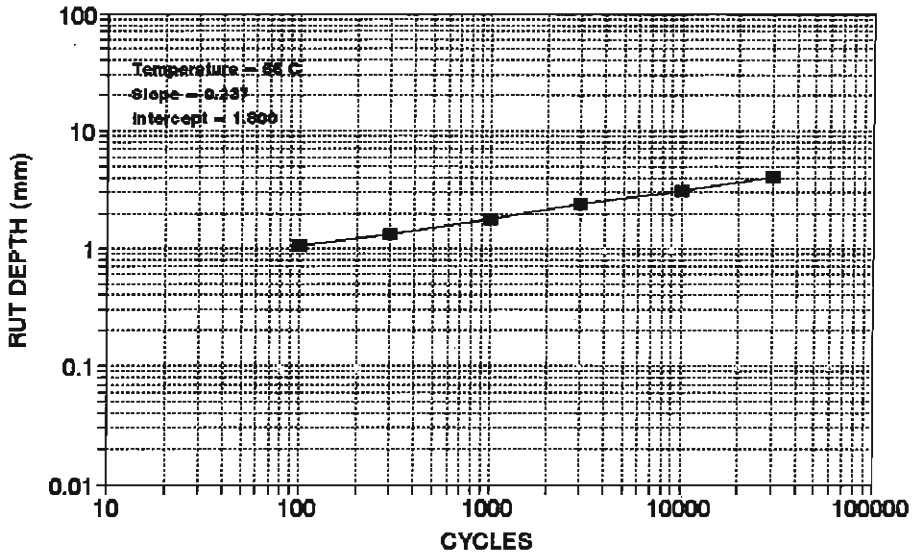

SITE 4, 50-mm Thick Field Sample

Actual Rut Depth

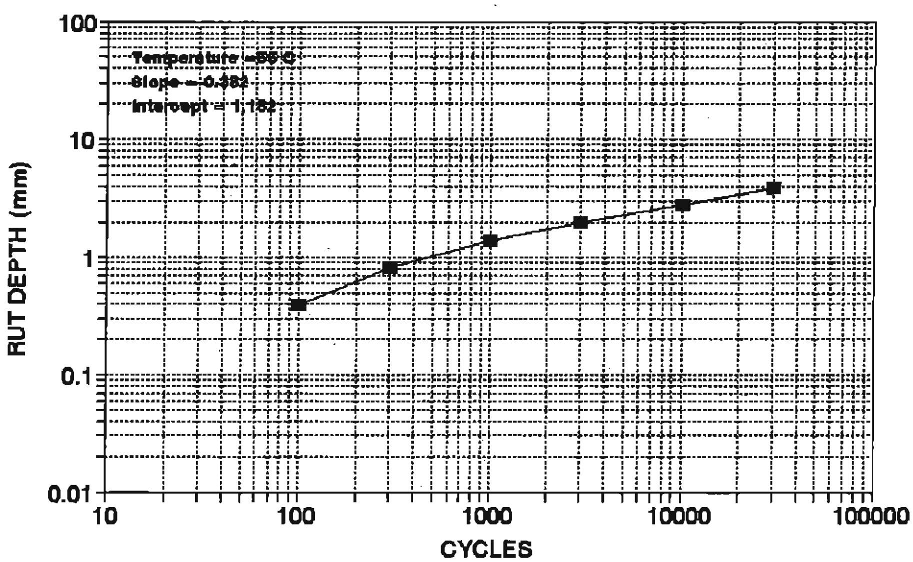

SITE 5, 50-mm Thick French Sample

Actual Rut Depth

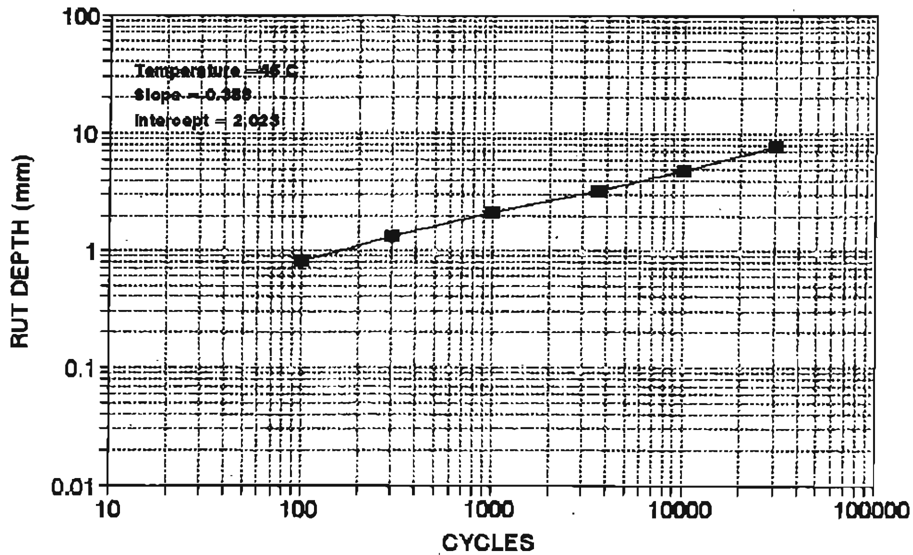

Site 5, 100-mm Thick French Sample

Actual Rut Depth

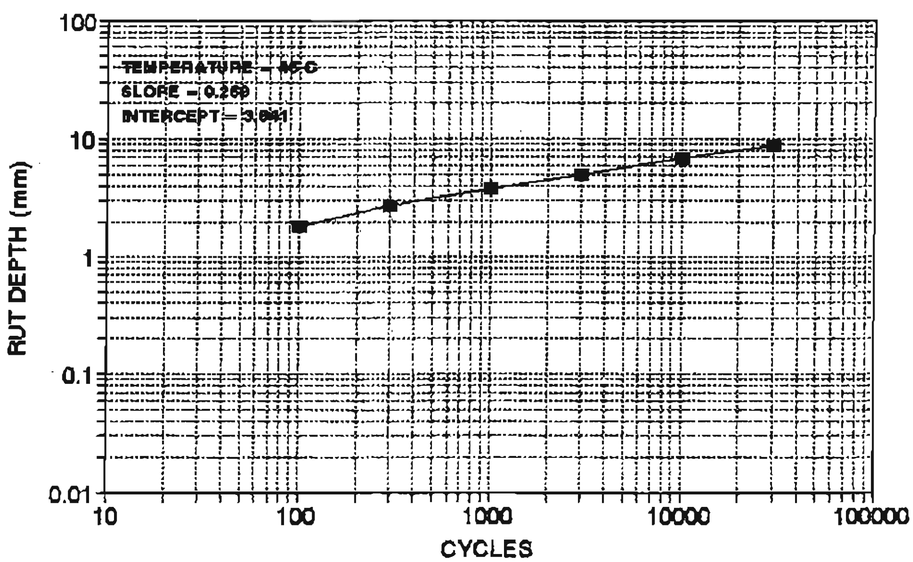

SITE 5, 100-mm Thick Linear Kneading

Actual Rut Depth

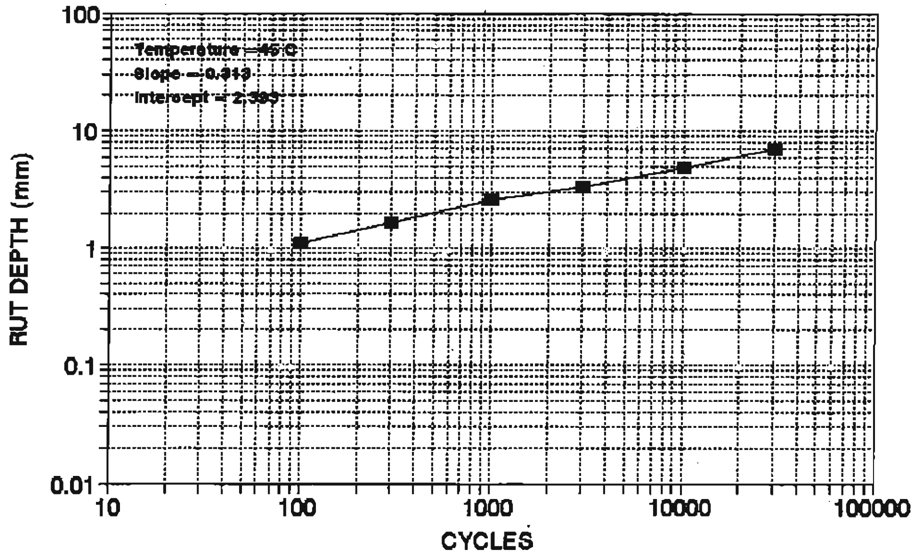

SITE 5, 50-mm Thick Field Sample

Actual Rut Depth

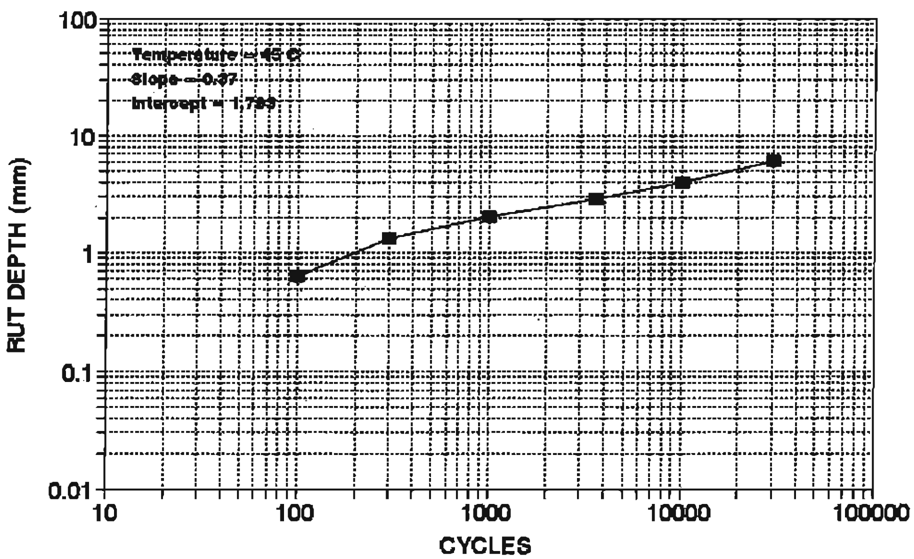

SITE 6, 50-mm Thick French Sample

Actual Rut Depth

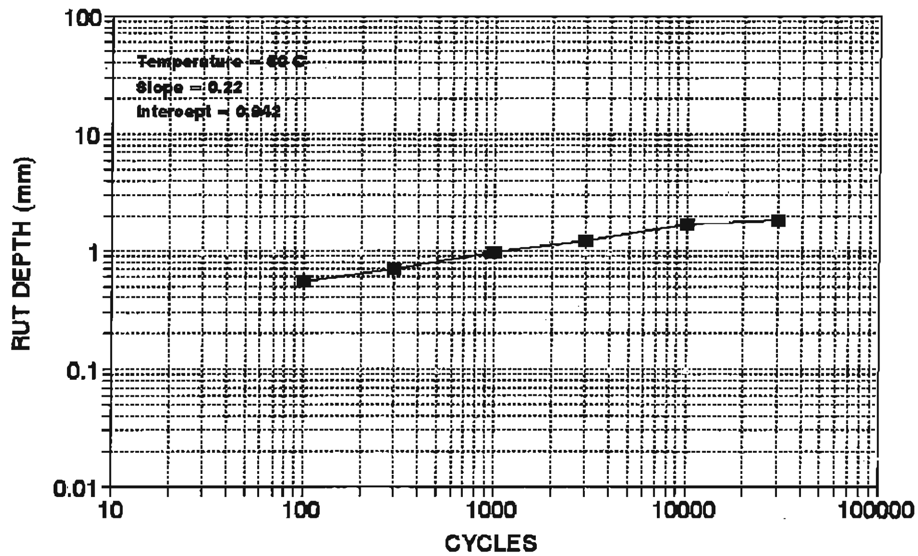

SITE 6, 100-mm Thick French Sample

Actual Rut Depth

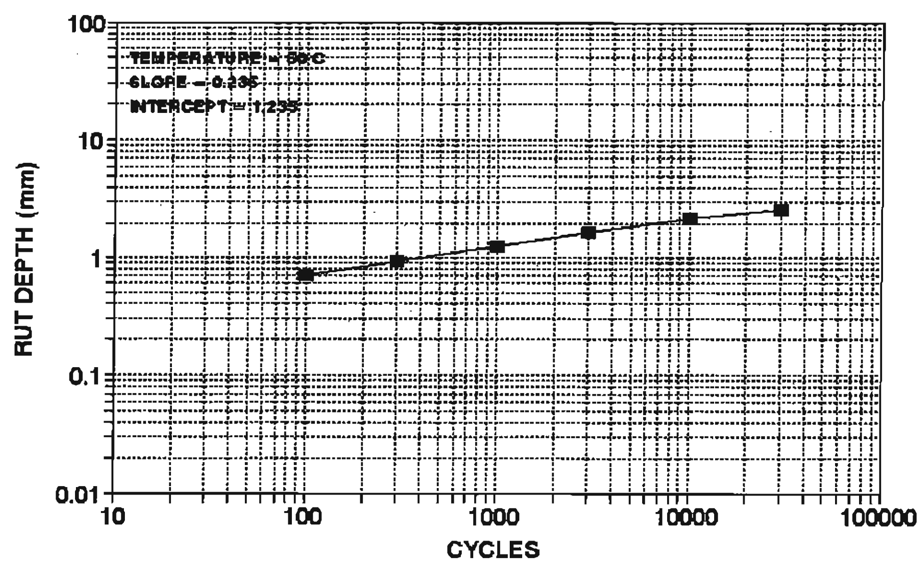

SITE 6, 100-mm Thick Linear Kneading

Actual Rut Depth

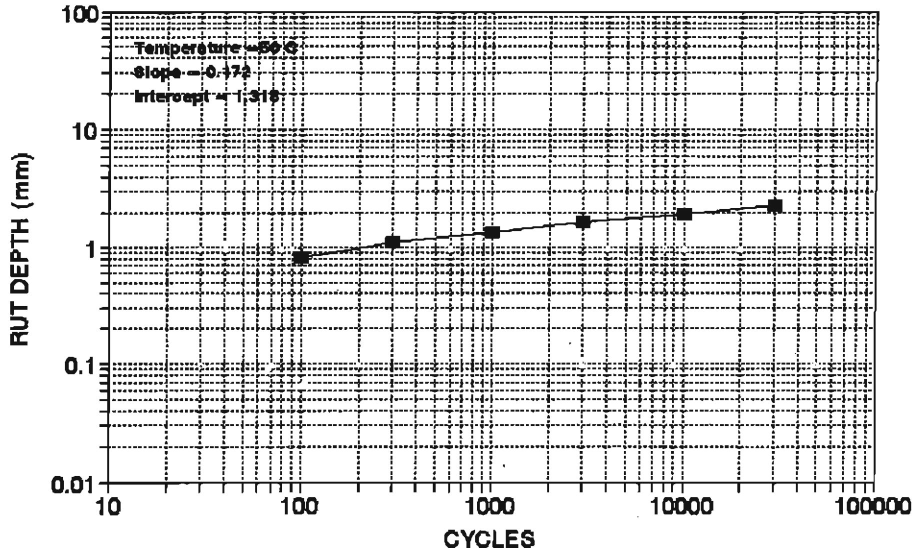

SITE 6, 50-mm Thick Field Sample

Actual Rut Depth

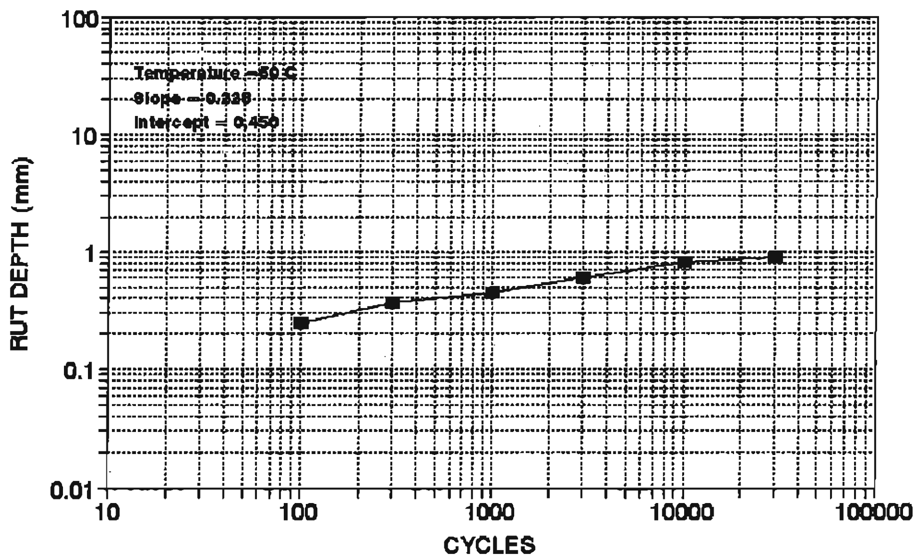

SITE 7, 50-mm Thick French Sample

Actual Rut Depth

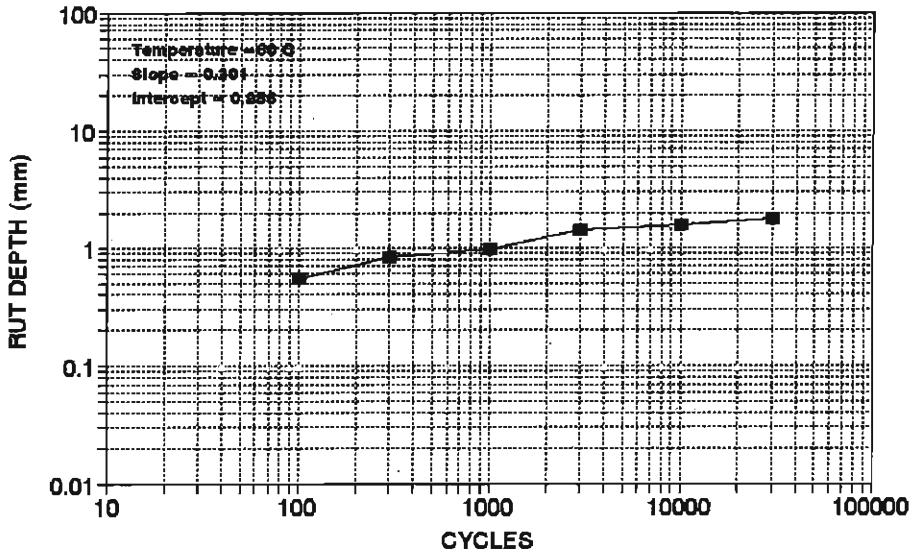

SITE 7, 100-mm Thick French Sample

Actual Rut Depth

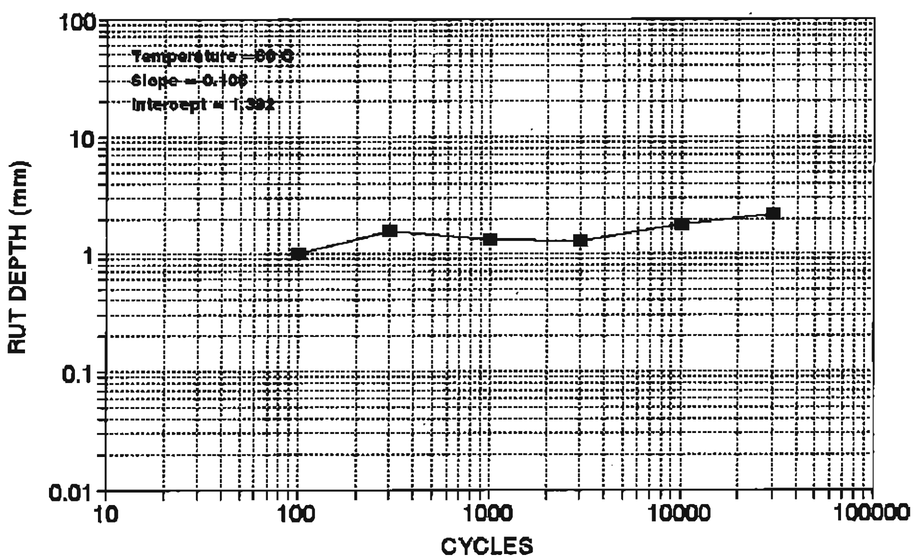

SITE 7, 100-mm Thick Linear Kneading

Actual Rut Depth

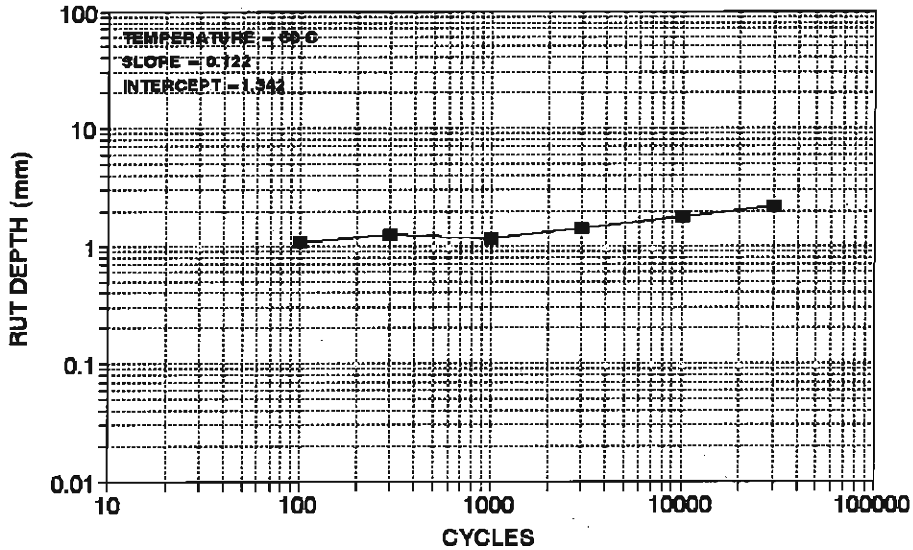

SITE 7, 50-mm Thick Field Sample

Actual Rut Depth

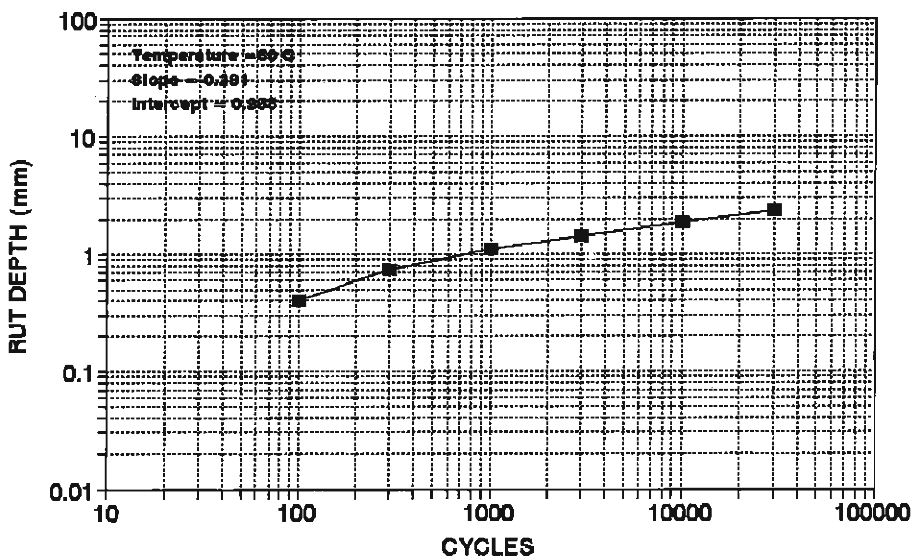

Appendix D

Hamburg Wheel-Tracking Results

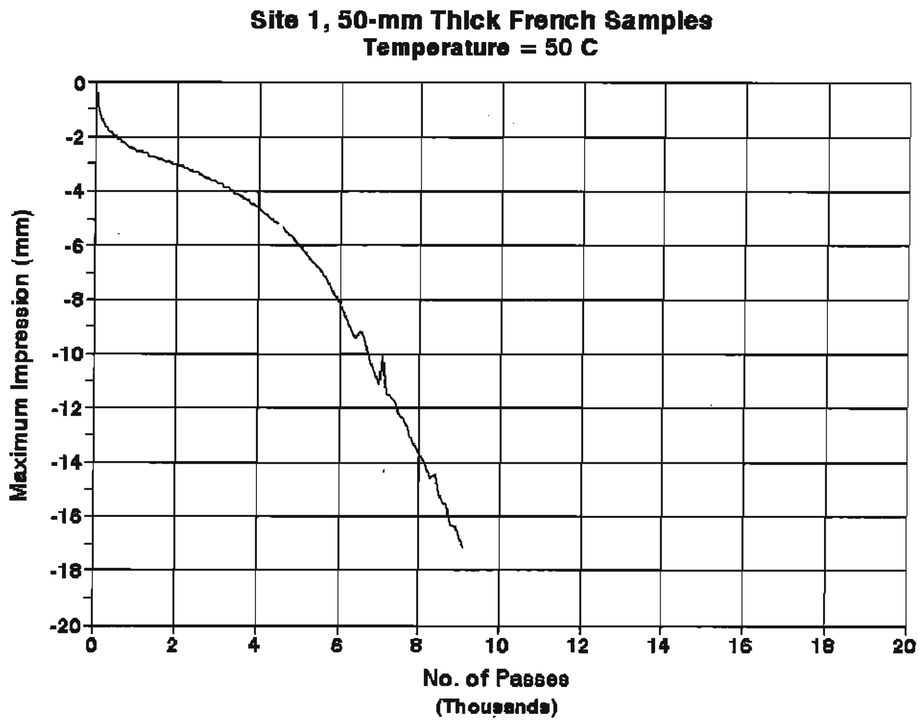
Site 1, 50-mm Thick French Samples
Temperature = 50 C
Maximum Impression (mm)
0
-2
-4
-6
-8
-10
-12
-14
-16
-18
-20
0
2
4
6
8
10
12
14
16
18
20
No. of Passes
(Thousands)

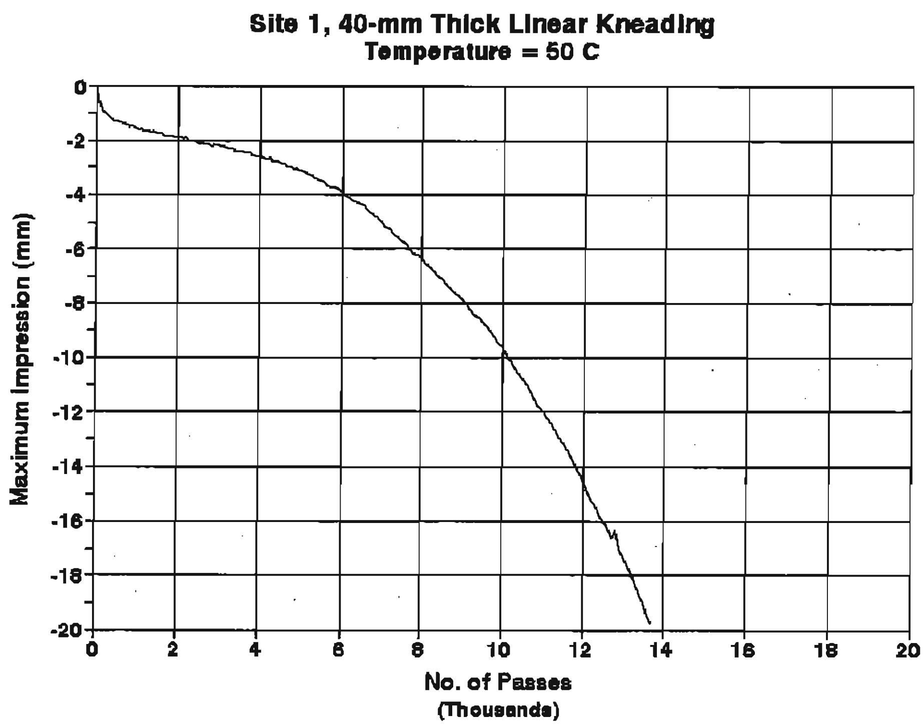
Site 1, 40-mm Thick Linear Kneading
Temperature = 50 C
Maximum Impression (mm)
0
-2
-4
-6
-8
-10
-12
-14
-16
-18
-20
0
2
4
6
8
10
12
14
16
18
20
No. of Passes
(Thousands)

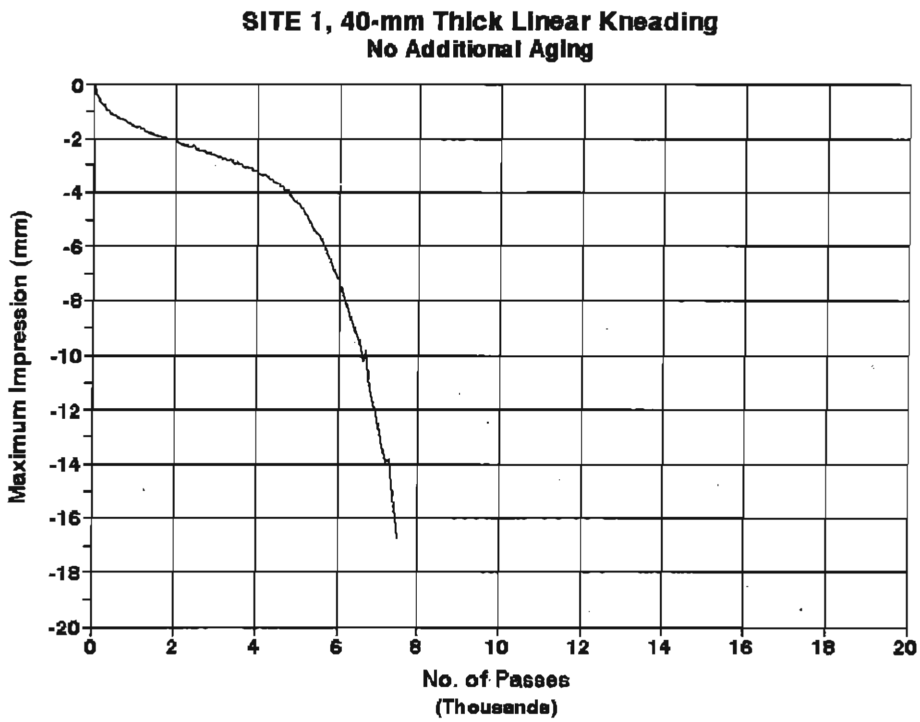
SITE 1, 40-mm Thick Linear Kneading
No Additional Aging
Maximum Impression (mm)
0
-2
-4
-6
-8
-10
-12
-14
-16
-18
-20
0
2
4
6
8
10
12
14
16
18
20
No. of Passes
(Thousands)

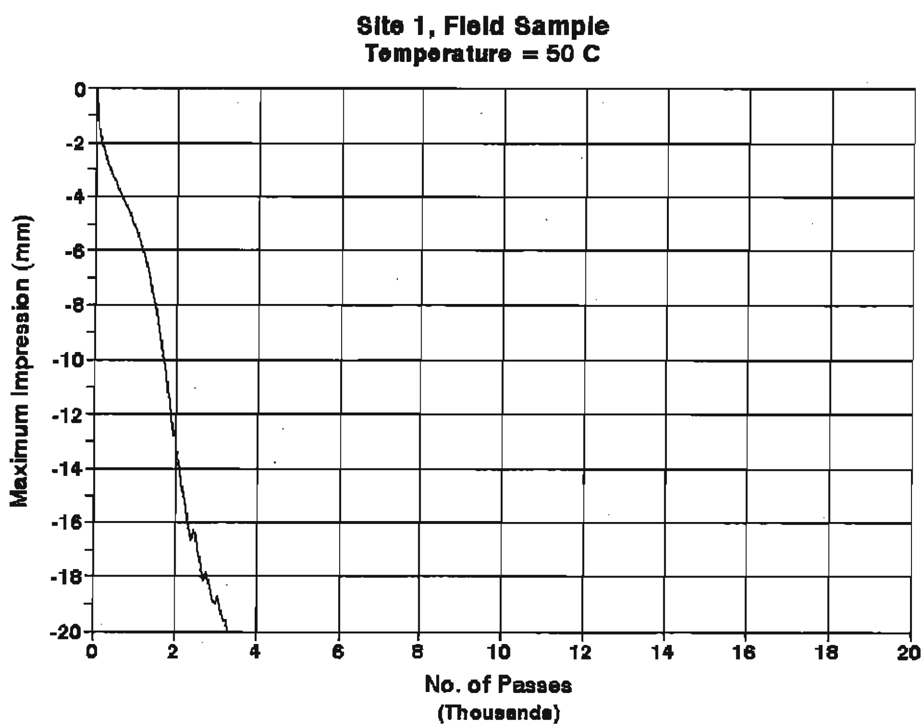
Site 1, Field Sample
Temperature = 50 C
Maximum Impression (mm)
0
-2
-4
-6
-8
-10
-12
-14
-16
-18
-20
0
2
4
6
8
10
12
14
16
18
20
No. of Passes
(Thousands)

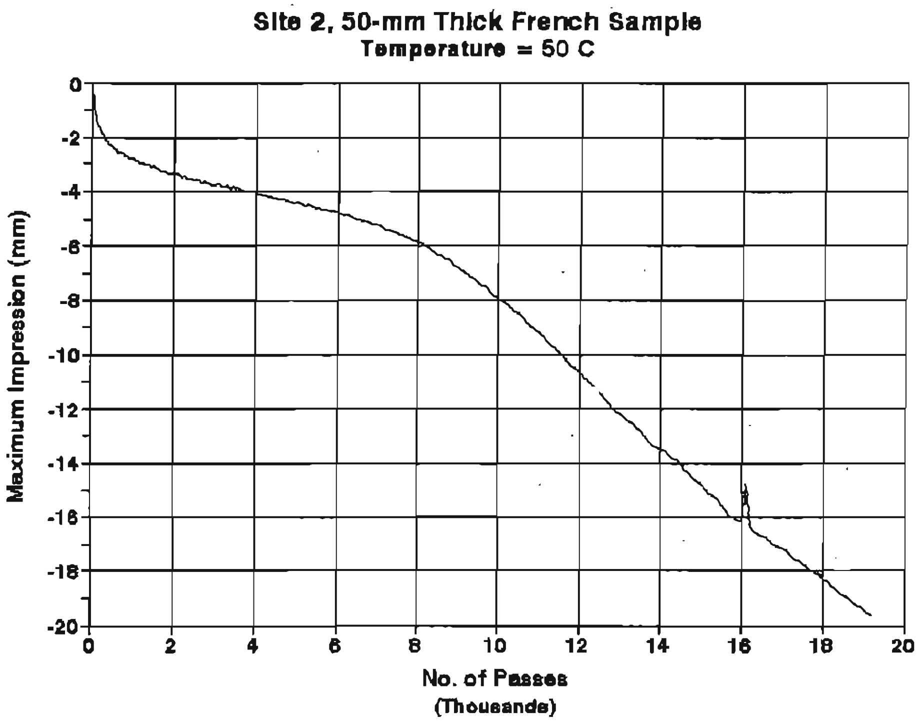
Site 2, 50-mm Thick French Sample
Temperature = 50 C
Maximum Impression (mm)
0
-2
-4
-6
-8
-10
-12
-14
-16
-18
-20
0
2
4
6
8
10
12
14
16
18
20
No. of Passes
(Thousands)

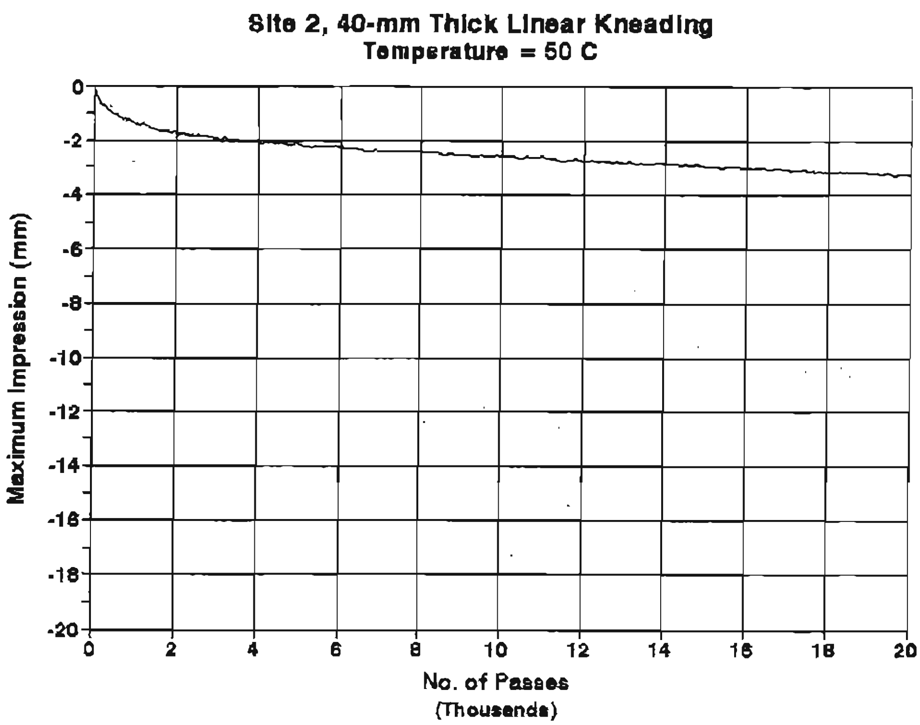
Site 2, 40-mm Thick Linear Kneading
Temperature = 50 C
Maximum Impression (mm)
0
-2
-4
-6
-8
-10
-12
-14
-16
-18
-20
0
2
4
6
8
10
12
14
16
18
20
No. of Passes
(Thousands)

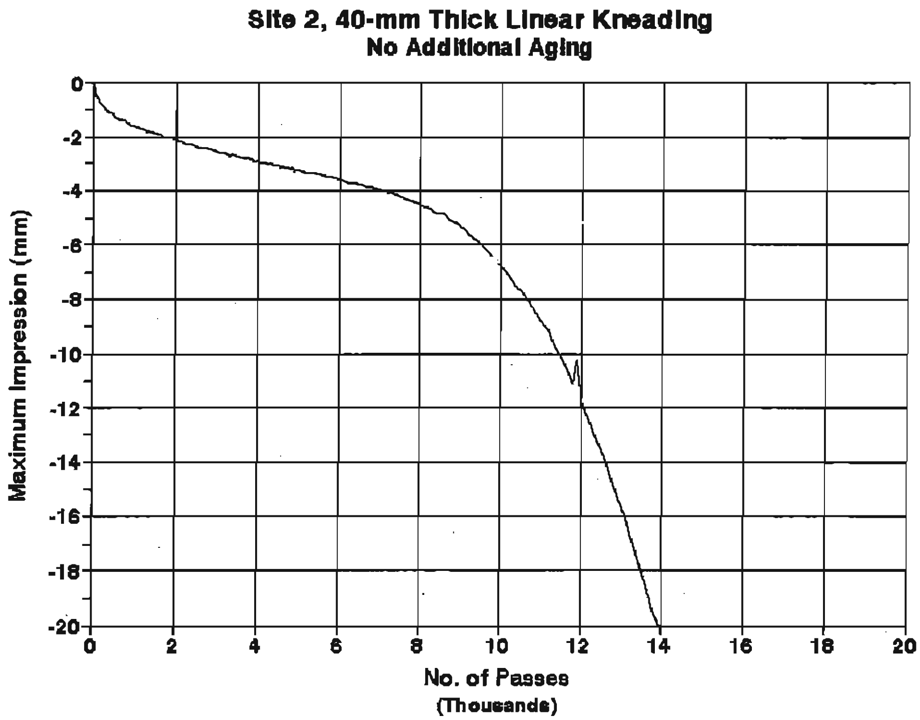
Site 2, 40-mm Thick Linear Kneading
No Additional Aging
Maximum Impression (mm)
0
-2
-4
-6
-8
-10
-12
-14
-16
-18
-20
0
2
4
6
8
10
12
14
16
18
20
No. of Passes
(Thousands)

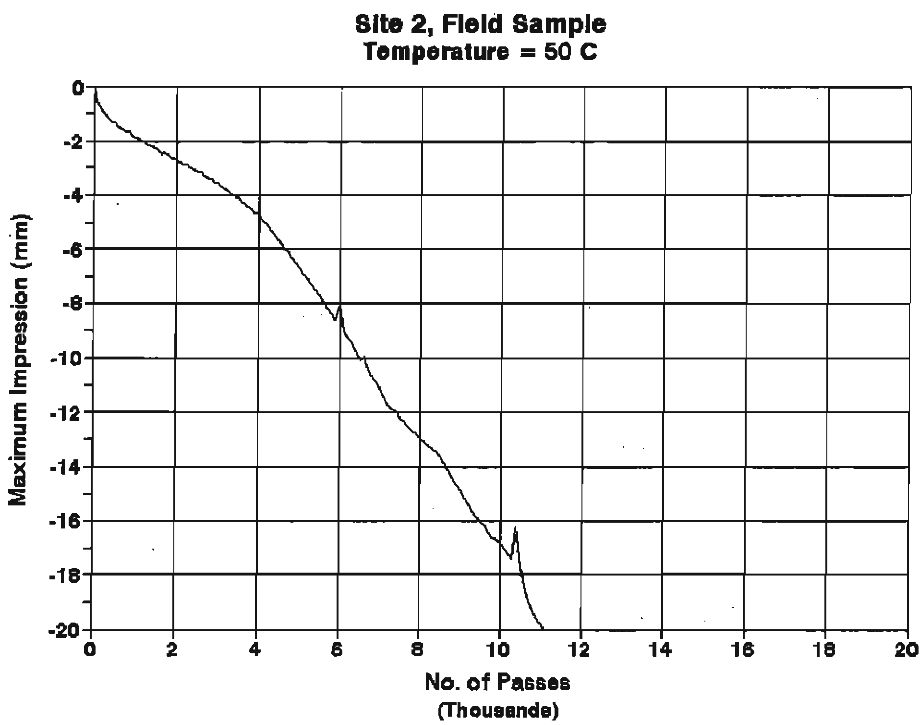
Site 2, Field Sample
Temperature = 50 C
Maximum Impression (mm)
0
-2
-4
-6
-8
-10
-12
-14
-16
-18
-20
0
2
4
6
8
10
12
14
16
18
20
No. of Passes
(Thousands)

Site 3, 50-mm Thick French Sample
Temperature = 50 C

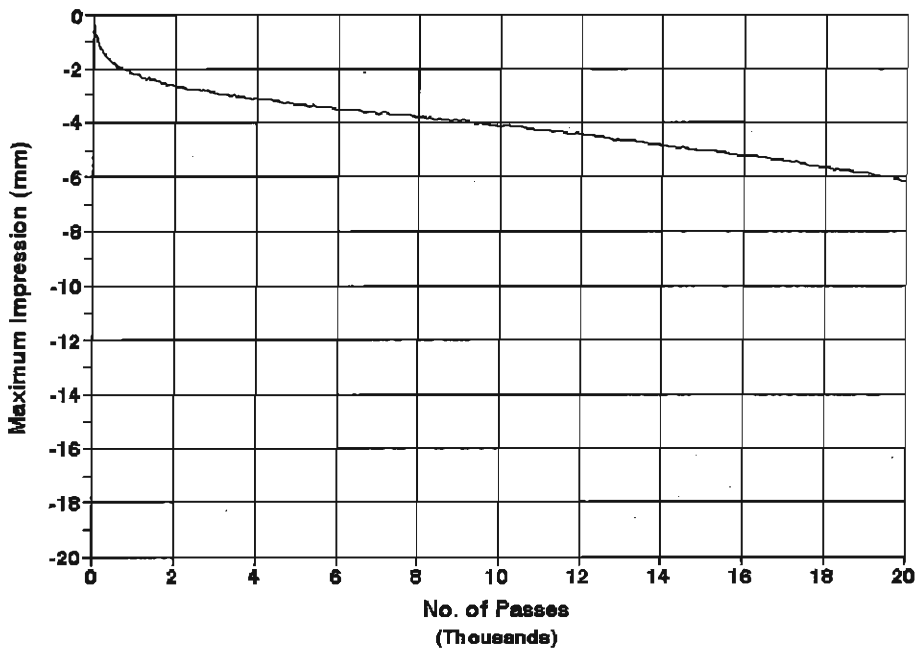

Site 3, 40-mm Thick Linear Kneading
Temperature = 50 C

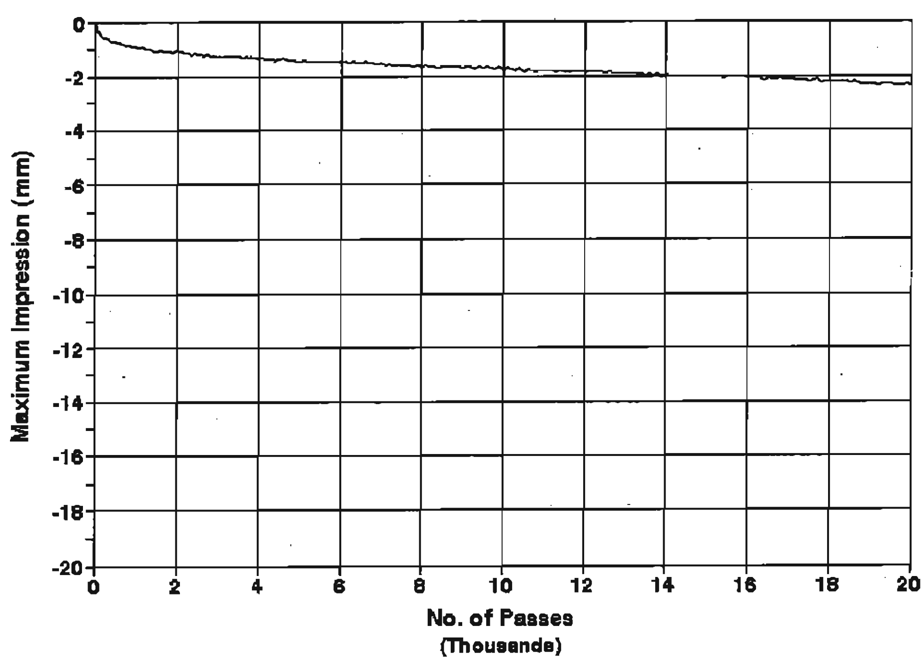

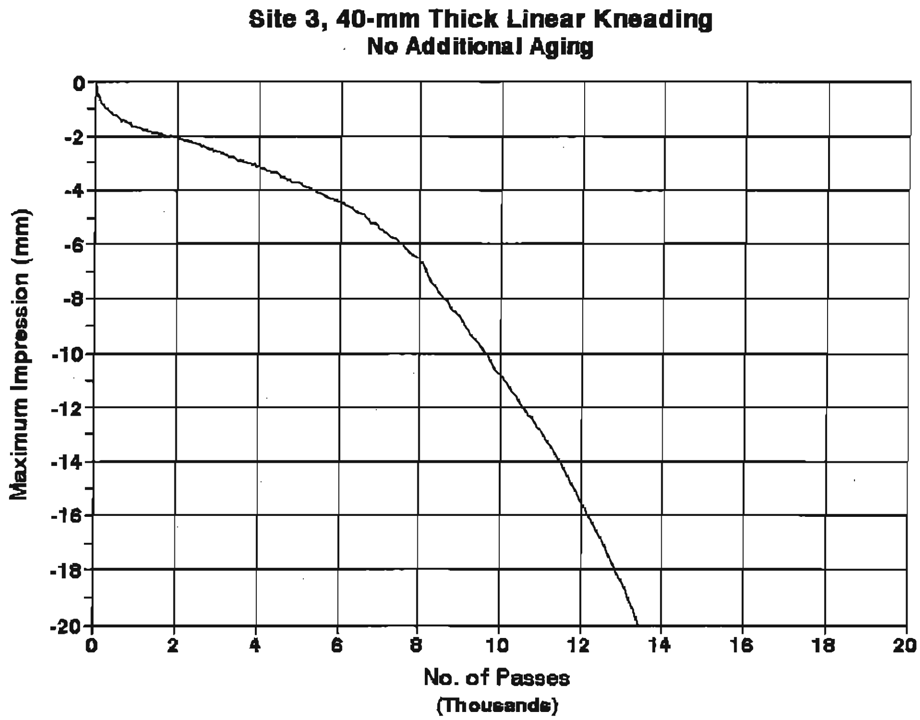
Site 3, 40-mm Thick Linear Kneading
No Additional Aging
Maximum Impression (mm)
0
-2
-4
-6
-8
-10
-12
-14
-16
-18
-20
0
2
4
6
8
10
12
14
16
18
20
No. of Passes
(Thousands)

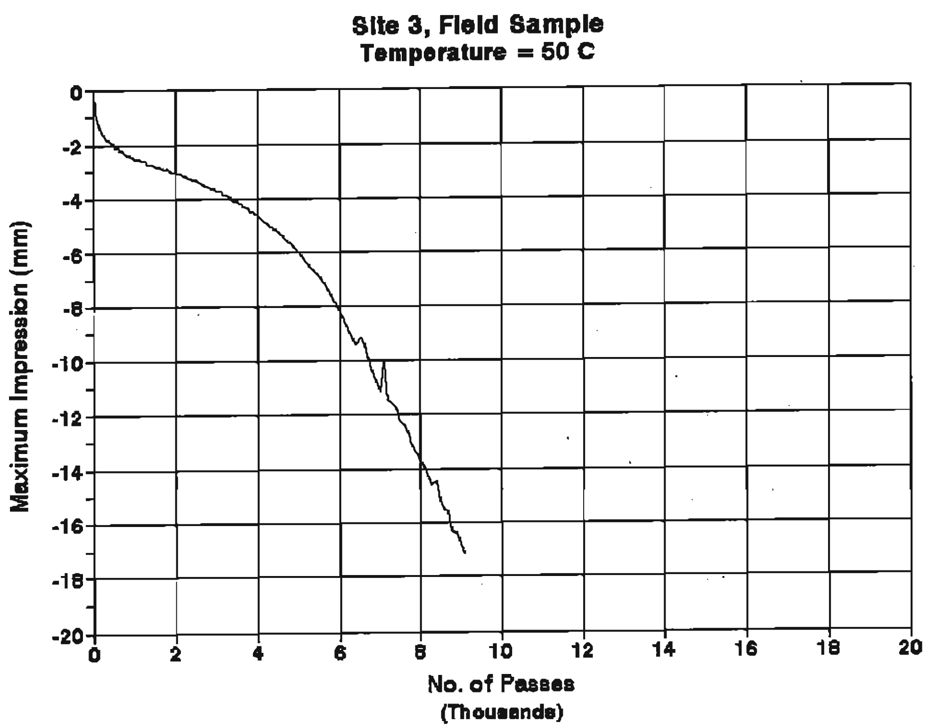
Site 3, Field Sample
Temperature = 50 C
Maximum Impression (mm)
0
-2
-4
-6
-8
-10
-12
-14
-16
-18
-20
0
2
4
6
8
10
12
14
16
18
20
No. of Passes
(Thousands)

Site 4, 50-mm Thick French Sample
Temperature = 45 C

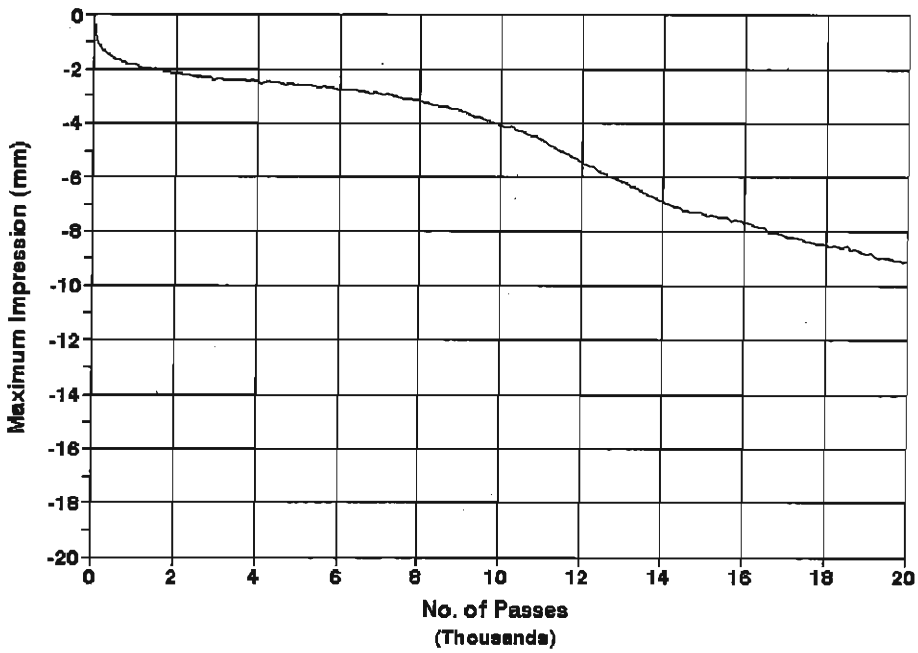

Site 4, 40-mm Thick Linear Kneading
Temperature = 45 C

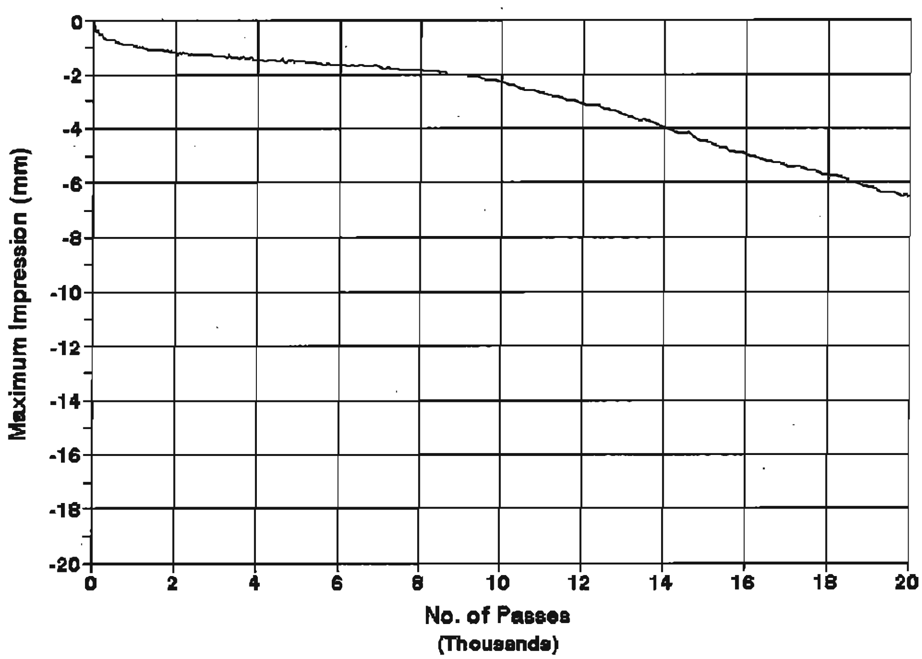

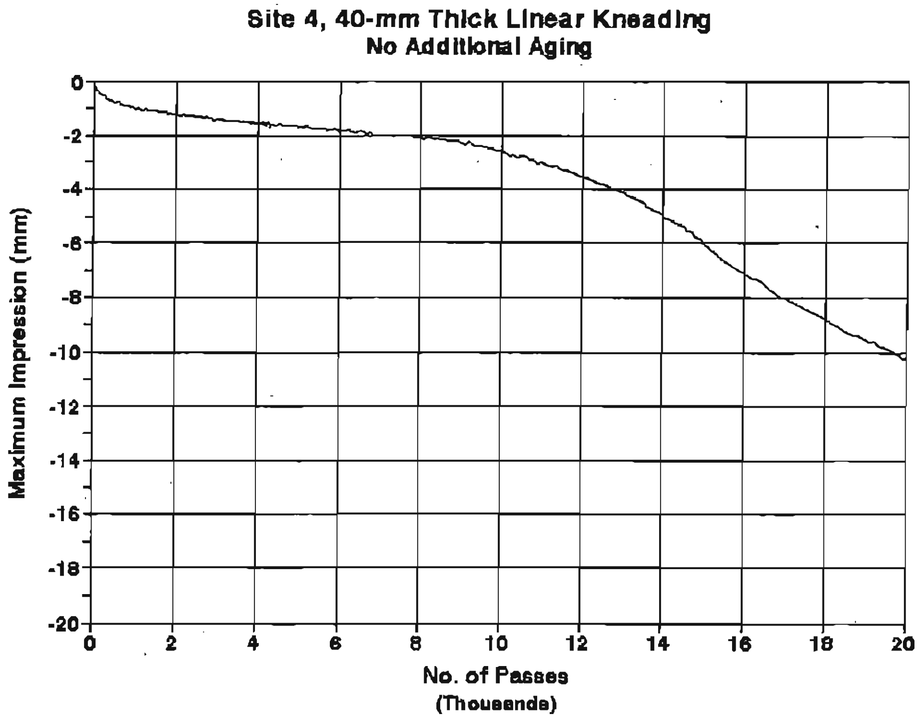
Site 4, 40-mm Thick Linear Kneading
No Additional Aging
Maximum Impression (mm)
0
-2
-4
-6
-8
-10
-12
-14
-16
-18
-20
0
2
4
6
8
10
12
14
16
18
20
No. of Passes
(Thousands)

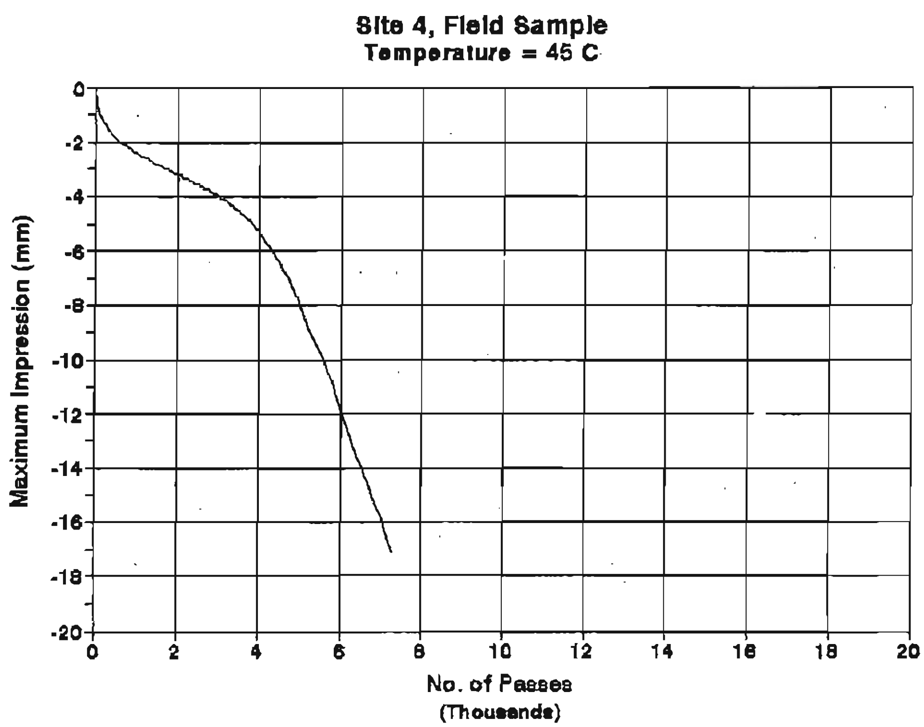
Site 4, Field Sample
Temperature = 45 C
Maximum Impression (mm)
0
-2
-4
-6
-8
-10
-12
-14
-16
-18
-20
0
2
4
6
8
10
12
14
16
18
20
No. of Passes
(Thousands)

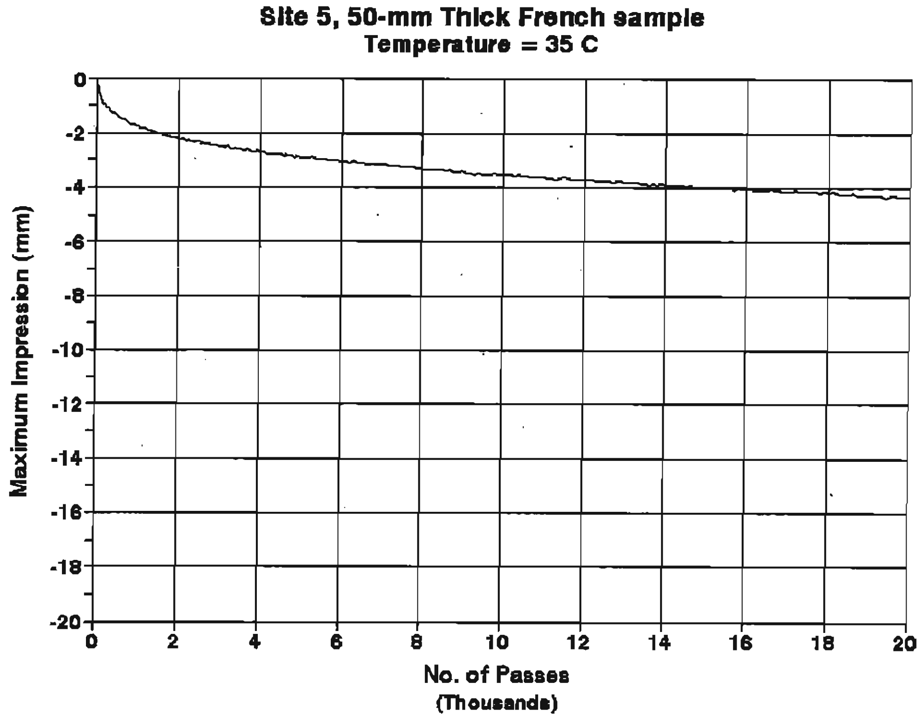

Site 5, 50-mm Thick French sample
Temperature = 35 C
Maximum Impression (mm)
0
-2
-4
-6
-8
-10
-12
-14
-16
-18
-20
0
2
4
6
8
10
12
14
16
18
20
No. of Passes
(Thousands)

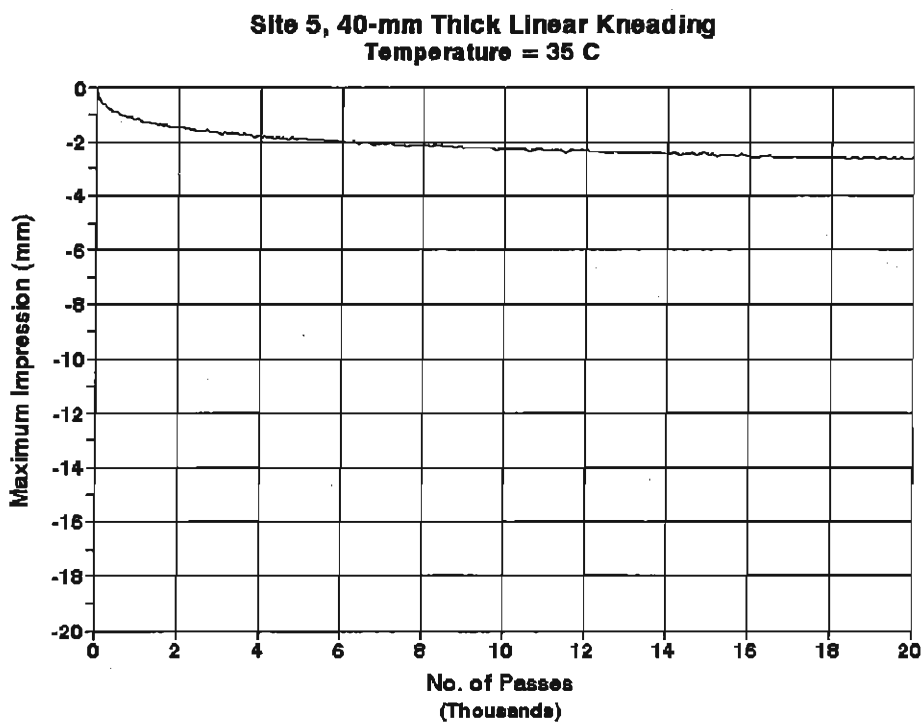

Site 5, 40-mm Thick Linear Kneading
Temperature = 35 C
Maximum Impression (mm)
0
-2
-4
-6
-8
-10
-12
-14
-16
-18
-20
0
2
4
6
8
10
12
14
16
18
20
No. of Passes
(Thousands)

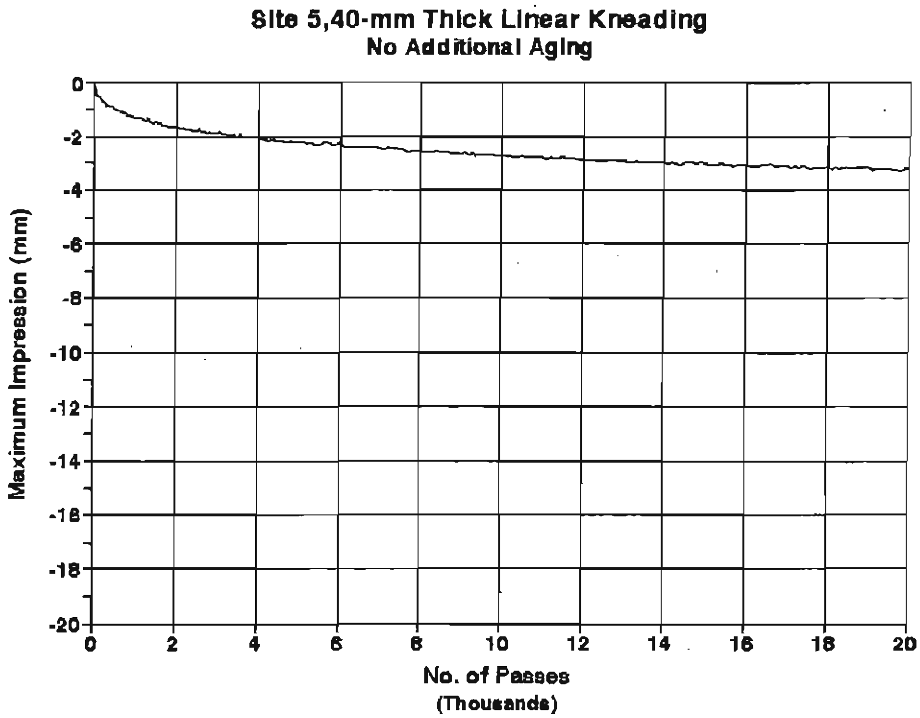
Site 5,40-mm Thick Linear Kneading
No Additional Aging
Maximum Impression (mm)
0
-2
-4
-6
-8
-10
-12
-14
-16
-18
-20
0
2
4
6
8
10
12
14
16
18
20
No. of Passes
(Thousands)

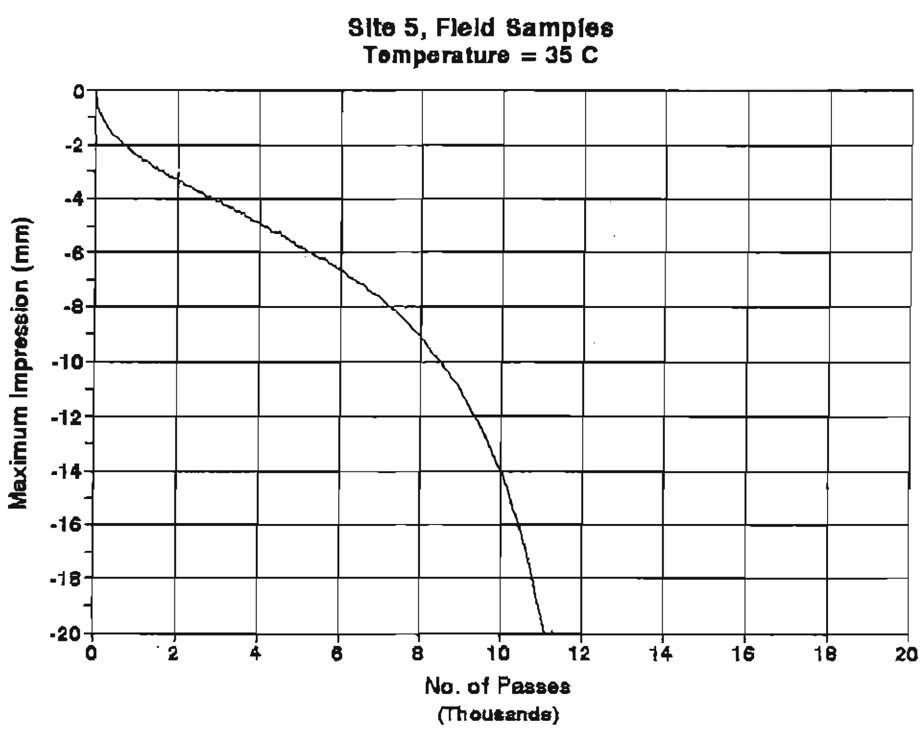
Site 5, Field Samples
Temperature = 35 C
Maximum Impression (mm)
0
-2
-4
-6
-8
-10
-12
-14
-16
-18
-20
0
2
4
6
8
10
12
14
16
18
20
No. of Passes
(Thousands)

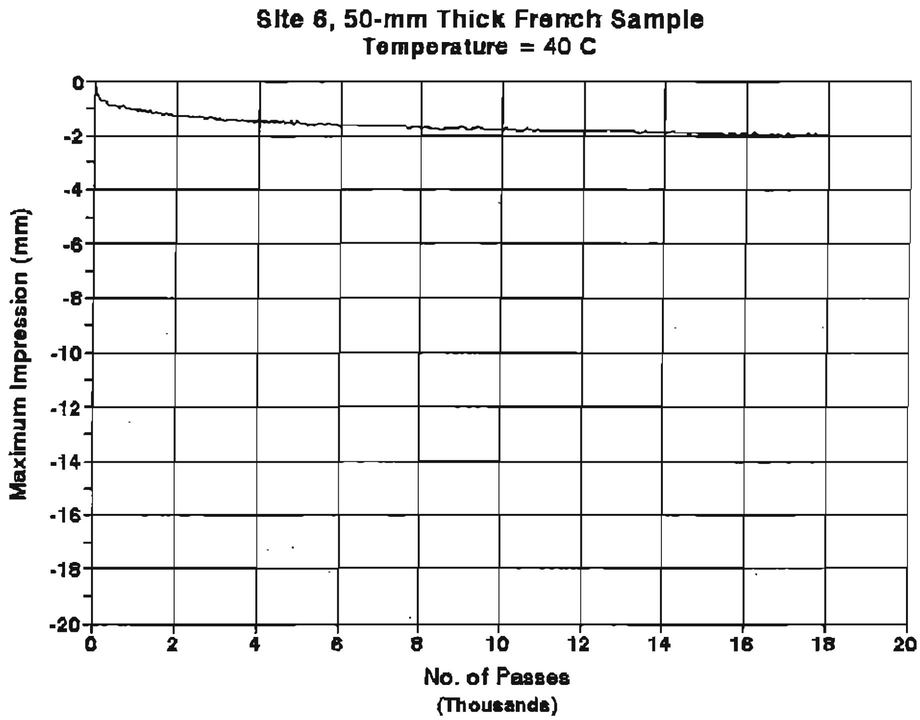
Site 6, 50-mm Thick French Sample
Temperature = 40 C
Maximum Impression (mm)
0
-2
-4
-6
-8
-10
-12
-14
-16
-18
-20
0
2
4
6
8
10
12
14
16
18
20
No. of Passes
(Thousands)

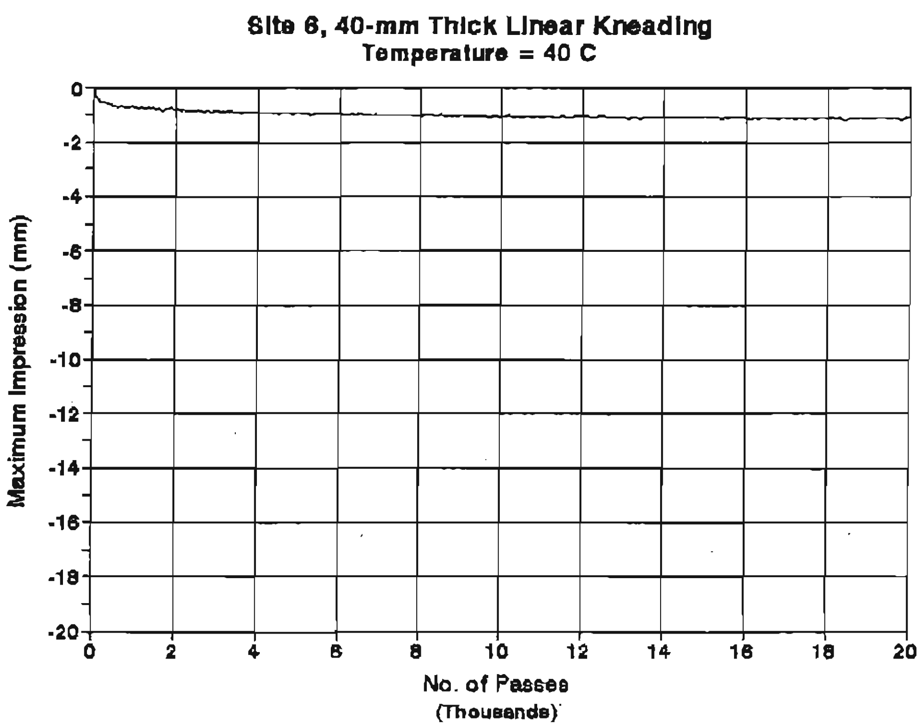
Site 6, 40-mm Thick Linear Kneading
Temperature = 40 C
Maximum Impression (mm)
0
-2
-4
-6
-8
-10
-12
-14
-16
-18
-20
0
2
4
6
8
10
12
14
16
18
20
No. of Passes
(Thousands)

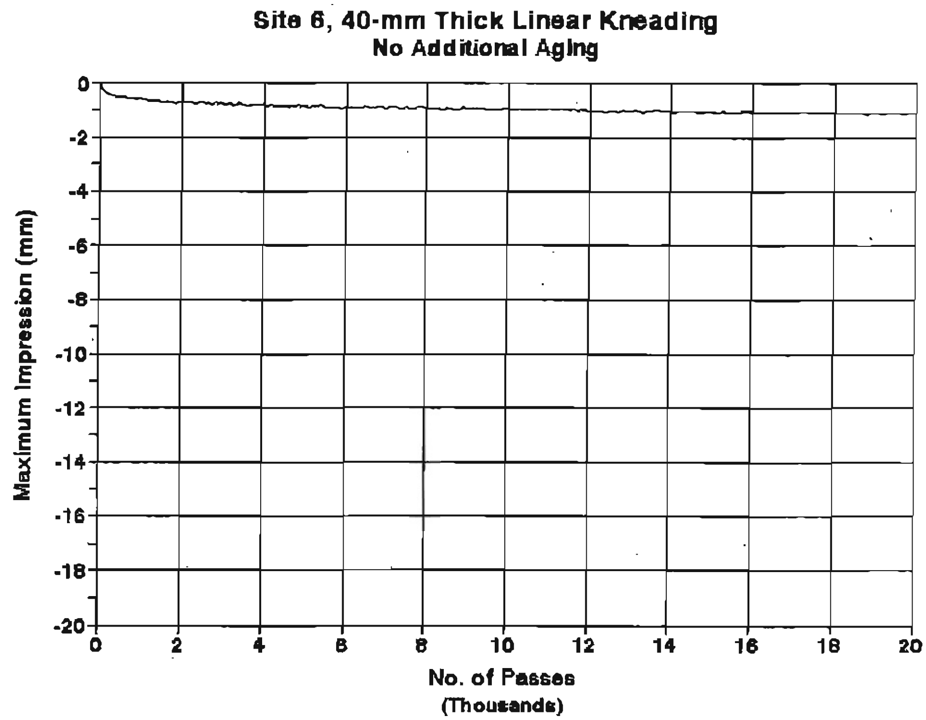
Site 6, 40-mm Thick Linear Kneading
No Additional Aging
Maximum Impression (mm)
0
-2
-4
-6
-8
-10
-12
-14
-16
-18
-20
0
2
4
6
8
10
12
14
16
18
20
No. of Passes
(Thousands)

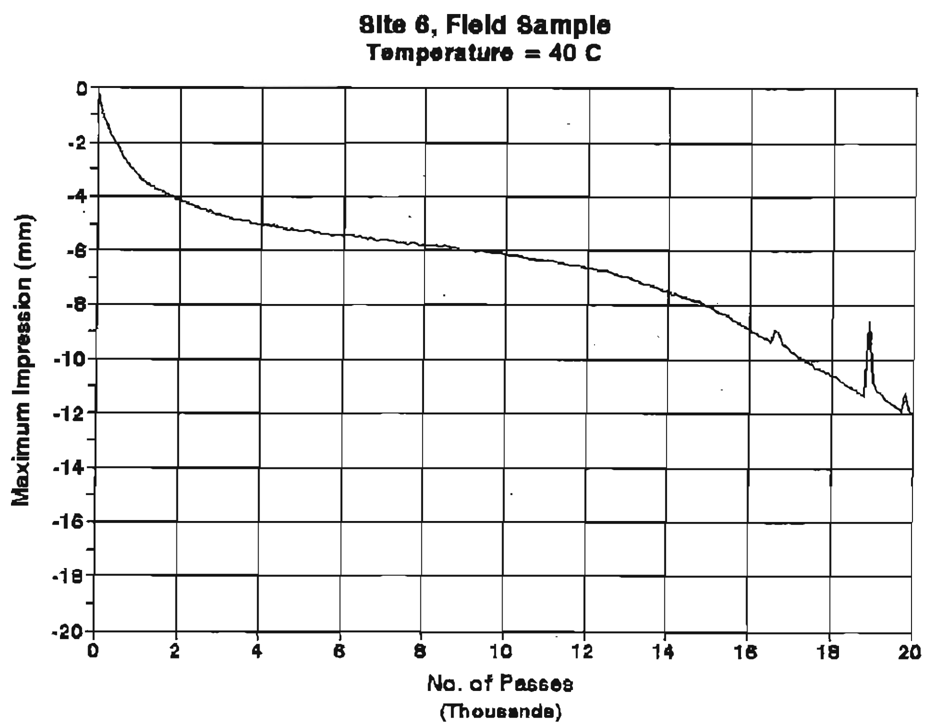
Site 6, Field Sample
Temperature = 40 C
Maximum Impression (mm)
0
-2
-4
-6
-8
-10
-12
-14
-16
-18
-20
0
2
4
6
8
10
12
14
16
18
20
No. of Passes
(Thousands)

Site 7, 50-mm Thick French Sample
Temperature = 50 C

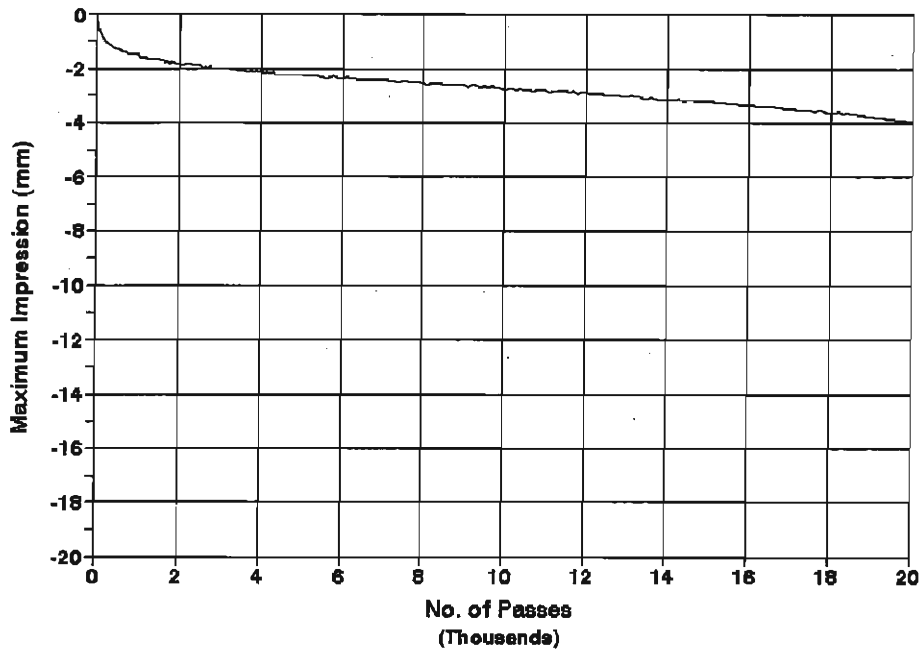

Site 7, 40-mm Thick Linear Kneading
Temperature = 50 C

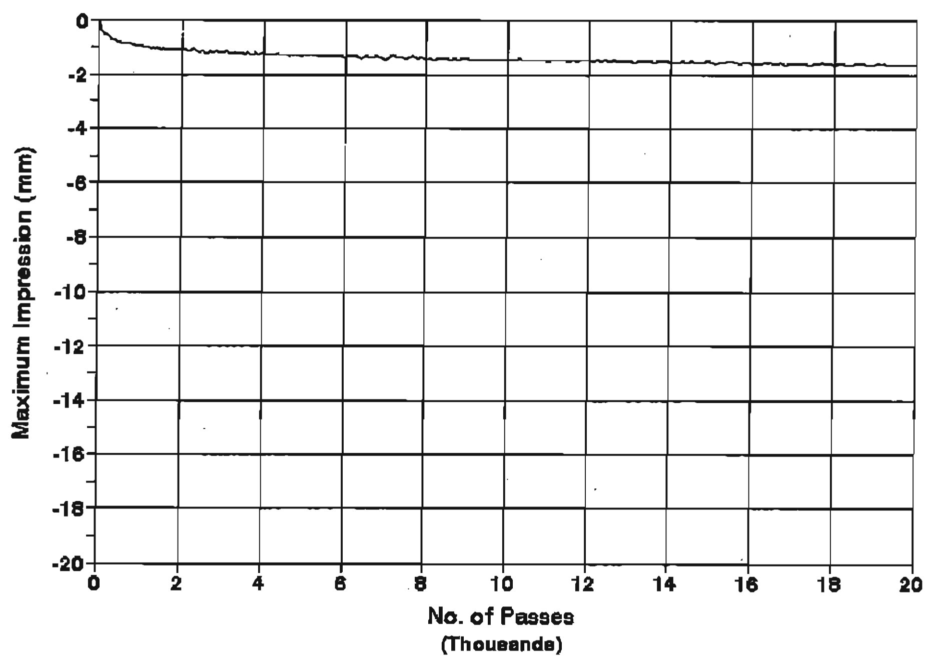

Site 7, 40-mm Thick Linear Kneading
No Additional Aging

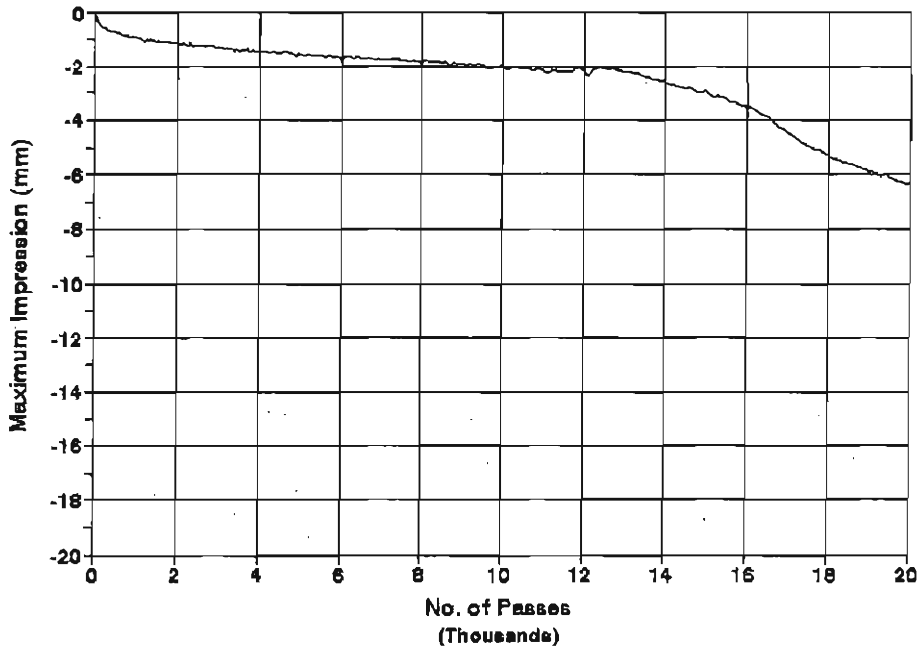

Site 7, Field Sample
Temperature = 50 C